Revista IRC, vol.01 nº.02 (set/2026) p.1–44

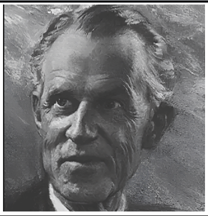

www.institutoroycarlson.org/revista

REVISTA IRC - Revista do Instituto Roy Carlson

TM **Instituto Roy Carlson** é uma instituição sem fins lucrativos dedicada a manter a memória técnica do concreto massa no Brasil e à difusão do conhecimento científico nos assuntos relacionados a barragens, com ênfase em concreto.

Calculation of thermally induced stresses in mass concrete considering creep with aging — Part I: formulation and analytical–numerical validation

Flávio Mamede Pereira Gomes[1]
Flávio Vasconcelos Souza[2]

[1] FM Furnas Engenharia / Instituto Roy Carlson; [2] Multimechanics (flaviovs@gmail.com); fundador; ex-Director of Siemens

Information
Received —
Accepted —
Published —

Keywords
mass concrete, creep with aging, thermal stresses, viscoelasticity, finite elements, analytical–numerical validation.

Abstract
This paper presents Part I — analytical–numerical — of the validation of a viscoelastic constitutive model: the incremental formulation of creep deformation *with aging* for the calculation of thermally induced stresses in mass-concrete structures. The starting point is the creep compliance obtained directly from tests (or from a rheological model fitted to it). Unlike the classical viscoelastic formulation of Zocher, Groves and Allen (1997), based on the relaxation moduli and without explicit aging, the present derivation operates on the creep compliance with aging, written as a Dirichlet–Prony series with coefficients that depend on the loading age. The strategy leads to a recursive algorithm in which the creep-strain increment at each time step separates into a known hereditary part and a part proportional to the current stress increment. The aging viscoelastic problem thus reduces, at each step, to an equivalent elastic problem suitable for finite-element implementation. The formulation is validated on analytical–numerical problems (in the manner of Zhu Bofang (2014) and Zocher et al. (1997), plane problems and a restrained slab). The numerical–experimental validation on site (VET / Santo Antônio HPP) is the subject of Part II.

1. Introduction

Concrete structures free to deform when subjected to a temperature change develop no internal forces: the material merely changes its dimensions, in proportion to the applied thermal gradient. In practice, however, restraints always exist — external (connection to the foundation or to other structures) and internal (gradient between the core and the surface, or connection to reinforcement). Such restraints give rise to internal forces which, if they exceed the concrete's resistance capacity, may lead to cracking.

In mass concrete, the temperature field is governed by the internal heat generation of hydration and by *Fourier's law* of heat conduction. Thermally induced stresses, in turn, depend not only on the temperature field but also on the evolution of the mechanical properties with age, especially *creep with aging*. Viscoelastic models with aging for mass concrete in dams — and the numerical resolution of those constitutive laws in the calculation of thermally induced stresses — were treated by Guedes and Gambale (1990) and by Gambale et al. (1992). Being a viscoelastic material, concrete relaxes the stresses in its interior over time, one of the main factors favoring the reduction of the cracking potential.

Quantitative prediction of this effect requires a constitutive model that:

1. starts from the creep function with aging (obtained by test, fitted to a Kelvin chain with aging);
2. admits arbitrary histories of stress and imposed strain (not only constant loading);
3. is numerically tractable in finite elements, without storing the entire stress history at each time step, since the problem is transient.

Zocher, Groves and Allen (1997) developed a three-dimensional finite-element formulation for linear orthotropic thermoviscoelastic media, converting the integral form based on the *relaxation moduli* (Dirichlet–Prony series) into an incremental recursive algebraic relation. That approach eliminates the storage problem typical of materials with memory and is effective for creep and relaxation under the hypothesis of constant rate within each step. However, (i) it operates on the *relaxation* function, not on the *creep* function; and (ii) it does not incorporate *aging* — the explicit dependence on loading age — which is essential in young concrete.

This article constitutes **Part I** of the validation of a viscoelastic constitutive model. The objective is to present, in detail, the derivation that allows the increment of creep strain with aging to be written in the form

$$\{\Delta\varepsilon^{cr}(t_n)\} = \{\eta_n\} + q_n\,[\mathbb{V}]\{\Delta\sigma_n\},$$

in which $\{\eta_n\}$ concentrates the history (known from the initial condition) and q_n is a scalar computable from the creep function and the current time interval. With this, the current stress increment enters in a manner analogous to a tangent elastic modulus, and the algorithm becomes implementable in the same sense as Zocher et al.'s formulation, yet anchored in the creep function with aging. The formulation is then validated against problems with known analytical solution, comparing that solution with the numerical solution of this implementation (in the manner of Zhu Bofang (2014) and Zocher et al. (1997), plane state and restrained slab). The numerical–experimental validation on an instrumentation campaign in class J mass concrete of the Log Spillway (VET) at Santo Antônio HPP, with processing of the strain results, is the subject of **Part II** (in preparation).

2. Governing equations of the mechanical problem

The task is to solve the equilibrium and compatibility equations of Classical Mechanics by the finite-element method. The governing equations are the equilibrium equations, the strain–displacement relations and the constitutive equation:

$$\nabla\cdot\boldsymbol{\sigma} + \rho f = \mathbf{0} \quad \text{or} \quad \sigma_{ji,\,j} + \rho f_i = 0,$$

$$\boldsymbol{\varepsilon} = \frac{1}{2}\left(\nabla u + (\nabla u)^T\right) \quad \text{or} \quad \varepsilon_{ij} = \frac{1}{2}(u_{i,\,j} + u_{j,\,i}),$$

$$\mathrm{d}\boldsymbol{\sigma}(x,\xi) = E(x,\xi)\,\mathbb{V}^{-1}\!:\mathrm{d}\Big(\boldsymbol{\varepsilon}(x,\xi) - \boldsymbol{\varepsilon}^{cr}(x,\xi) - \boldsymbol{\varepsilon}^{th}(x,\xi) - \boldsymbol{\varepsilon}^{shr}(x,\xi) - \boldsymbol{\varepsilon}^{pl}(x,\xi)\Big).$$

The classical boundary conditions read:

$$\begin{aligned} u &= \widehat{u} && \text{on } \partial\Omega_1, \\ T = \boldsymbol{\sigma}\cdot n &= \widehat{T} && \text{on } \partial\Omega_2. \end{aligned}$$

The creep strain, in hereditary integral form, is:

$$\boldsymbol{\varepsilon}^{cr}(x,\xi) = \int_0^{\xi} \mathbb{D}\left(x,\xi,\xi'\right) : \frac{\partial\boldsymbol{\sigma}(x,\xi')}{\partial\xi'}\,\mathrm{d}\xi'.$$

The integral is understood as a Stieltjes integral: any discontinuities (steps) in the stress history contribute discrete terms, made explicit in Section 4.

In the formulation above, f is the body force, T is the surface traction, n is the outward unit normal to the boundary, and ρ is the mass density. It is understood that $\boldsymbol{\varepsilon}$, $\boldsymbol{\sigma}$ and the constitutive operators are functions of the point x. Henceforth, for notational convenience, x is omitted wherever there is no ambiguity.

Note that the instantaneous elastic part is carried by the modulus $E(\xi)$ of the incremental constitutive equation itself; the strain $\boldsymbol{\varepsilon}^{cr}$ is therefore creep *proper*, that is, the time-dependent part, without the $1/E$ contribution. This separation fixes the meaning of the function D adopted throughout the text (Section 3).

Considering, on the basis of extensive literature, that for concrete Poisson's ratio may be treated as simply elastic (time-independent), the fourth-order tensor $\mathbb{D}$ specializes as the product of a fourth-order tensor $\mathbb{V}$, independent of time and age, by a scalar D dependent on time and age (creep function with aging):

$$\boldsymbol{\varepsilon}^{cr}(\xi) = \mathbb{V}\colon \int_0^{\xi} D(\xi, \xi') \, \frac{\partial \boldsymbol{\sigma}(\xi')}{\partial \xi'} \, \mathrm{d}\xi'.$$

The arguments ξ and ξ' are the *equivalent time* (or reduced time or pseudo-time), which describes the influence of temperature on the viscoelastic kinetics:

$$\xi = \xi(t) \equiv \int_0^t \frac{1}{a_T} \, \mathrm{d}\tau, \qquad \xi' = \xi(t') \equiv \int_0^{t'} \frac{1}{a_T} \, \mathrm{d}\tau,$$

where $a_T = a_T[\theta(\tau)]$ is the *shift factor* of the time–temperature superposition principle. This factor may be expressed, for example, by an Arrhenius equation in terms of the activation energy.

For the isotropic material, the tensor $\mathbb{V}$ admits the matrix representation (Voigt notation)

$$[\mathbb{V}] = \begin{bmatrix} 1 & -\nu & -\nu & 0 & 0 & 0 \\ -\nu & 1 & -\nu & 0 & 0 & 0 \\ -\nu & -\nu & 1 & 0 & 0 & 0 \\ 0 & 0 & 0 & 2(1+\nu) & 0 & 0 \\ 0 & 0 & 0 & 0 & 2(1+\nu) & 0 \\ 0 & 0 & 0 & 0 & 0 & 2(1+\nu) \end{bmatrix}.$$

The notation $[\mathbb{V}]$ (Voigt matrix form) and $\mathbb{V}$ (tensor form), as well as the practical rule for directional projections and rosette assembly, are detailed in a note.[1]

3. Creep compliance with aging

The total creep compliance $J(t, z)$, which for notational convenience, but without loss of generality, we keep as t and z, is a strain per unit stress at time t due to a load applied at age z. One may write:

$$J(t, z) = \frac{1}{E(z)} + D(t, z),$$

where $1/E(z)$ is the instantaneous elastic part (modulus at the loading age) and $D(t, z)$ is the creep part proper, that is, the time-dependent part. A generalized rheological model (Kelvin chain with aging), adjustable to tests, is:

$$D(t, z) = \sum_{i=1}^{N} D_i(z) \left[1 - e^{-(t-z)/\tau_i} \right].$$

The coefficients $D_i(z)$ depend on the loading age (aging); the retardation times τ_i fix the *spectrum* of the chain ($i = 1, ..., N$). Note that D depends on the current instant t only through the load duration $t - z$, whereas the age z enters twice: in the duration and in the amplitudes $D_i(z)$. A usual aging form of the amplitudes is

$$D_i(z) = a_i + b_i\, e^{-z/c_i}.$$

or, if needed for a better fit to the data, with several aging time constants,

$$D_i(z) = a_i + \sum_{j=1}^{M_i} b_{i,j}\, e^{-z/c_{i,j}},$$

in which the constant term a_i stands outside the sum (the constant parts of each exponential aggregate into a single a_i) and M_i is the number of aging exponentials of the i-th unit.

It is shown in Annex B that this form allows an exact calculation for the creep model known as B4 (Bažant, Hubler and Wendner, 2015): the amplitudes have a closed-form spectral representation, and the dependence on z turns out to be a superposition of decaying exponentials with non-negative coefficients and no constant term. The same annex treats the admissibility constraints that the creep surface must satisfy and the scope of the regression alternative.

In terms of reduced time, the same structure appears as:

$$D(\xi, \xi') = \sum_{i=1}^{N} D_i(\xi') \left[1 - e^{-(\xi - \xi')/\tau_i}\right],$$

with the τ_i measured on the reduced-time scale. To avoid overloading the notation, the derivation that follows is written in t and z; the reading in reduced time is obtained by substituting $t \to \xi$ and $z \to \xi'$, with no algebraic change whatsoever.

4. Constitutive equation of creep and objective of the derivation

Under uniaxial loading (or, in 3D, accounting for $\mathbb{V}$), the creep strain at time t is:

$$\varepsilon^{cr}(t) = \Delta\sigma_0\, D(t, t_0) + \int_{t_0}^{t} D(t, z)\, \frac{\partial \sigma}{\partial z}\, \mathrm{d}z.$$

In three dimensions,

$$\{\varepsilon^{cr}(t)\} = [\mathbb{V}]\{\Delta\sigma_0\}\, D(t, t_0) + \int_{t_0}^{t} D(t, z)\, [\mathbb{V}] \left\{ \frac{\partial \sigma}{\partial z} \right\} \mathrm{d}z.$$

The stress history admits the representation:

$$\sigma(t) = H(t - t_0)\, \Delta\sigma_0 + \int_{t_0}^{t} \frac{\partial \sigma}{\partial z}\, \mathrm{d}z,$$

where H is the Heaviside function and $\Delta\sigma_0$ is the initial stress jump at t_0 (if any). The first term of the creep strain is therefore the discrete contribution of that step, and the integral covers only the continuous part of the history. The objective of the derivation is to show that the *increment* of creep strain in the step ending at t_n can be written in the form:

$$\{\Delta\varepsilon^{cr}(t_n)\} = \{\eta_n\} + q_n\,[\mathbb{V}]\{\Delta\sigma_n\}.$$

This form allows, at each step, treating $\{\eta_n\}$ as a known "imposed strain" and absorbing $q_n\mathbb{V}$ into the tangent stiffness matrix (or into the incremental constitutive operator).

5. Time discretization and creep increment

In a typical interval, t_n is the generic instant and $\Delta t_n = t_n - t_{n-1}$. One adopts the same hypothesis as in Zocher et al.'s formulation — one of the most innovative aspects of that formulation and responsible for the large efficiency gain in the implementation — taking the stress rate as constant within the interval, and thereafter integrating the stress history analytically within that interval.

$$\frac{\partial\sigma}{\partial z} = \text{const.} = \frac{\Delta\sigma_n}{\Delta t_n} \quad \text{for } z \in [t_{n-1}, t_n].$$

The creep-strain increment is, by definition,

$$\{\Delta\varepsilon_n^{cr}\} = \{\varepsilon^{cr}(t_n)\} - \{\varepsilon^{cr}(t_{n-1})\}.$$

Substituting the constitutive equation at t_n and at t_{n-1},

$$\begin{aligned}\{\Delta\varepsilon_n^{cr}\} = [\mathbb{V}]\{\Delta\sigma_0\}\,D(t_n, t_0) + \int_{t_0}^{t_n} D(t_n, z)\,[\mathbb{V}]\left\{\frac{\partial\sigma}{\partial z}\right\}\mathrm{d}z \\ -\,[\mathbb{V}]\{\Delta\sigma_0\}\,D(t_{n-1}, t_0) - \int_{t_0}^{t_{n-1}} D(t_{n-1}, z)\,[\mathbb{V}]\left\{\frac{\partial\sigma}{\partial z}\right\}\mathrm{d}z.\end{aligned}$$

The operator $[\mathbb{V}]$ is constant and multiplies equally the terms at t_n and at t_{n-1}, and may be factored out whenever convenient.

5.1 Introduction of $\Delta D_{n,z}$ and splitting of the integrals

We define

$$\Delta D_{n,z} = D(t_n, z) - D(t_{n-1}, z).$$

Splitting the integration interval $[t_0, t_n]$ into $[t_0, t_{n-1}]$ and $[t_{n-1}, t_n]$, and regrouping, one obtains:

$$\begin{aligned}\{\Delta\varepsilon_n^{cr}\} = [\mathbb{V}]\{\Delta\sigma_0\}\,\Delta D_{n,0} + \int_{t_{n-1}}^{t_n} D(t_n, z)\,[\mathbb{V}]\left\{\frac{\partial\sigma}{\partial z}\right\}\mathrm{d}z \\ +\int_{t_0}^{t_{n-1}} \Delta D_{n,z}\,[\mathbb{V}]\left\{\frac{\partial\sigma}{\partial z}\right\}\mathrm{d}z,\end{aligned}$$

with the abbreviated notation $\Delta D_{n,0} \equiv \Delta D_{n,z}\big|_{z=t_0} = D(t_n, t_0) - D(t_{n-1}, t_0)$.

Calling the first integral I and the second II,

$$I = \int_{t_{n-1}}^{t_n} D(t_n, z)\,[\mathbb{V}]\left\{\frac{\partial \sigma}{\partial z}\right\} \mathrm{d}z,$$

$$II = \int_{t_0}^{t_{n-1}} \Delta D_{n,z}\,[\mathbb{V}]\left\{\frac{\partial \sigma}{\partial z}\right\} \mathrm{d}z,$$

one has:

$$\{\Delta\varepsilon_n^{cr}\} = [\mathbb{V}]\{\Delta\sigma_0\}\,\Delta D_{n,0} + I + II.$$

The part I involves only the current interval and, therefore, the unknown increment $\{\Delta\sigma_n\}$. The part II and the term in $\Delta D_{n,0}$ involve only the history up to t_{n-1} and will be gathered into $\{\eta_n\}$.

5.2 Evaluation of integral I (current-step contribution)

Inserting the creep series into I,

$$I = \int_{t_{n-1}}^{t_n} \sum_{i=1}^{N} D_i(z)\left[1 - e^{-(t_n - z)/\tau_i}\right][\mathbb{V}]\left\{\frac{\partial \sigma}{\partial z}\right\} \mathrm{d}z.$$

Defining:

$$D_{i,n}^{*} = D_i\left(t_n - \frac{\Delta t_n}{2}\right),$$

that is, a constant value of D_i between t_{n-1} and t_n, evaluated at mid-interval, and knowing that $[\mathbb{V}]$ is independent of z and that $\{\partial\sigma/\partial z\}$ is also constant in that interval, and recalling that summation and integration commute ($\int \sum = \sum \int$), it follows that:

$$I = [\mathbb{V}]\frac{\{\Delta\sigma_n\}}{\Delta t_n}\sum_{i=1}^{N} D_{i,n}^{*}\int_{t_{n-1}}^{t_n}\left[1 - e^{-(t_n - z)/\tau_i}\right]\mathrm{d}z.$$

The antiderivative of the integrand with respect to z is:

$$\int\left[1 - e^{-(t_n - z)/\tau_i}\right]\mathrm{d}z = z - \tau_i\, e^{-(t_n - z)/\tau_i},$$

since

$$\frac{\mathrm{d}}{\mathrm{d}z}e^{-(t_n - z)/\tau_i} = \frac{1}{\tau_i}\,e^{-(t_n - z)/\tau_i}.$$

Evaluating between t_{n-1} and t_n,

$$\left[z - \tau_i\, e^{-(t_n - z)/\tau_i}\right]_{t_{n-1}}^{t_n} = \Delta t_n - \tau_i\left(1 - e^{-\Delta t_n/\tau_i}\right).$$

Therefore,

$$I = [\mathbb{V}]\frac{\{\Delta\sigma_n\}}{\Delta t_n}\sum_{i=1}^{N} D^*_{i,n}\left[\Delta t_n - \tau_i\left(1 - e^{-\Delta t_n/\tau_i}\right)\right],$$

that is,

$$I = q_n\,[\mathbb{V}]\{\Delta\sigma_n\},$$

with

$$q_n = \sum_{i=1}^{N} D^*_{i,n}\left[1 - \frac{\tau_i}{\Delta t_n}\left(1 - e^{-\Delta t_n/\tau_i}\right)\right].$$

The scalar q_n depends only on the creep function (via D_i and τ_i) and on the step Δt_n: it is known *before* solving the equilibrium of step n. Two control limits, useful in numerical verification of the implementation, are worth recording: as $\Delta t_n/\tau_i \to 0$ the bracket tends to $\Delta t_n/(2\tau_i)$, and $q_n \to 0$; as $\Delta t_n/\tau_i \to \infty$ the bracket tends to 1, and $q_n \to \sum_i D^*_{i,n}$, that is, to the asymptotic creep of the chain.

5.3 Evaluation of integral II (past history) and auxiliary variables $\omega_{i,n}$

To evaluate II, one first simplifies $\Delta D_{n,z}$:

$$\begin{aligned}\Delta D_{n,z} &= D(t_n, z) - D(t_{n-1}, z)\\ &= \textstyle\sum_{i=1}^{N} D_i(z)\left[1 - e^{-(t_n - z)/\tau_i}\right] - \sum_{i=1}^{N} D_i(z)\left[1 - e^{-(t_{n-1} - z)/\tau_i}\right]\\ &= \textstyle\sum_{i=1}^{N} D_i(z)\left[-e^{-(t_n - z)/\tau_i} + e^{-(t_{n-1} - z)/\tau_i}\right].\end{aligned}$$

Factoring out $e^{-(t_{n-1} - z)/\tau_i}$,

$$\Delta D_{n,z} = \sum_{i=1}^{N} D_i(z)\, e^{-(t_{n-1} - z)/\tau_i}\left[1 - e^{-\Delta t_n/\tau_i}\right],$$

since

$$e^{-(t_n - z)/\tau_i} = e^{-(t_{n-1} - z)/\tau_i}\, e^{-\Delta t_n/\tau_i}.$$

Integral II becomes:

$$II = \int_{t_0}^{t_{n-1}} \sum_{i=1}^{N} D_i(z)\, e^{-(t_{n-1} - z)/\tau_i}\left[1 - e^{-\Delta t_n/\tau_i}\right][\mathbb{V}]\left\{\frac{\partial\sigma}{\partial z}\right\}\,\mathrm{d}z.$$

Commuting sum and integral, and taking out the z-independent term (the factor $1 - e^{-\Delta t_n/\tau_i}$),

$$II = \sum_{i=1}^{N} \left[1 - e^{-\Delta t_n/\tau_i}\right] \{\omega_{i,n}\},$$

where the auxiliary variable is defined:

$$\{\omega_{i,n}\} = \int_{t_0}^{t_{n-1}} D_i(z)\, e^{-(t_{n-1}-z)/\tau_i} [\mathbb{V}] \left\{ \frac{\partial \sigma}{\partial z} \right\} \mathrm{d}z.$$

Note that $\{\omega_{i,n}\}$ integrates the history up to t_{n-1}, not up to t_n: it is a quantity known at the beginning of step n.

5.3.1 Recurrence relation for $\{\omega_{i,n}\}$

At the previous instant,

$$\{\omega_{i,n-1}\} = \int_{t_0}^{t_{n-2}} D_i(z)\, e^{-(t_{n-2}-z)/\tau_i} [\mathbb{V}] \left\{ \frac{\partial \sigma}{\partial z} \right\} \mathrm{d}z.$$

Multiplying both sides by $e^{-\Delta t_{n-1}/\tau_i}$,

$$\begin{aligned} \{\omega_{i,n-1}\}\, e^{-\Delta t_{n-1}/\tau_i} &= \int_{t_0}^{t_{n-2}} D_i(z)\, e^{-(t_{n-2}-z)/\tau_i}\, e^{-\Delta t_{n-1}/\tau_i} [\mathbb{V}] \left\{ \frac{\partial \sigma}{\partial z} \right\} \mathrm{d}z \\ &= \int_{t_0}^{t_{n-2}} D_i(z)\, e^{-(t_{n-1}-z)/\tau_i} [\mathbb{V}] \left\{ \frac{\partial \sigma}{\partial z} \right\} \mathrm{d}z, \end{aligned}$$

since $t_{n-2} + \Delta t_{n-1} = t_{n-1}$.
Splitting the integration interval of $\{\omega_{i,n}\}$ into $[t_0, t_{n-2}]$ and $[t_{n-2}, t_{n-1}]$,

$$\begin{aligned} \{\omega_{i,n}\} = &\int_{t_{n-2}}^{t_{n-1}} D_i(z)\, e^{-(t_{n-1}-z)/\tau_i} [\mathbb{V}] \left\{ \frac{\partial \sigma}{\partial z} \right\} \mathrm{d}z \\ &+ \int_{t_0}^{t_{n-2}} D_i(z)\, e^{-(t_{n-1}-z)/\tau_i} [\mathbb{V}] \left\{ \frac{\partial \sigma}{\partial z} \right\} \mathrm{d}z. \end{aligned}$$

The second part is exactly $\{\omega_{i,n-1}\}e^{-\Delta t_{n-1}/\tau_i}$. From the first, the z-independent terms are taken out of the integral (in particular $[\mathbb{V}]\{\Delta\sigma_{n-1}\}/\Delta t_{n-1}$ and the mid-interval value $D^*_{i,n-1}$), yielding:

$$\{\omega_{i,n}\} = [\mathbb{V}] \frac{\{\Delta \sigma_{n-1}\}}{\Delta t_{n-1}} D^*_{i,n-1} \int_{t_{n-2}}^{t_{n-1}} e^{-(t_{n-1}-z)/\tau_i}\, \mathrm{d}z + \{\omega_{i,n-1}\}\, e^{-\Delta t_{n-1}/\tau_i}.$$

The antiderivative of $e^{-(t_{n-1}-z)/\tau_i}$ is $\tau_i\, e^{-(t_{n-1}-z)/\tau_i}$. Evaluating between t_{n-2} and t_{n-1},

$$\left[\tau_i\, e^{-(t_{n-1}-z)/\tau_i}\right]_{t_{n-2}}^{t_{n-1}} = \tau_i \left(1 - e^{-\Delta t_{n-1}/\tau_i}\right).$$

Hence,

$$\{\omega_{i,n}\} = [\mathbb{V}]\{\Delta\sigma_{n-1}\}\, D^*_{i,n-1}\frac{\tau_i}{\Delta t_{n-1}}\left(1 - e^{-\Delta t_{n-1}/\tau_i}\right) + \{\omega_{i,n-1}\}\, e^{-\Delta t_{n-1}/\tau_i}.$$

This is the *recurrence relation*: only the stress increment of the previous step, the previous auxiliary value and the parameters of the creep series are needed. It is not necessary to reintegrate from t_0.

For $n = 1$, the interval $[t_0, t_{n-1}]$ is empty and integral II vanishes; consequently

$$\{\omega_{i,1}\} = \mathbf{0}.$$

It should be emphasized that the recurrence involves only the increments $\{\Delta\sigma_{n-1}\}$ with $n-1 \geq 1$, that is, the continuous part of the history. The initial step $\{\Delta\sigma_0\}$ is entirely represented by the term in $\Delta D_{n,0}$ and is never introduced into $\{\omega_{i,n}\}$.

5.4 Final expression for $\{\eta_n\}$ and the creep increment

Gathering the term in $\Delta D_{n,0}$ with integral II,

$$\begin{aligned}\{\eta_n\} &= [\mathbb{V}]\{\Delta\sigma_0\}\,\Delta D_{n,0} + II \\ &= [\mathbb{V}]\{\Delta\sigma_0\}\textstyle\sum_{i=1}^N D_i(t_0)\, e^{-(t_{n-1}-t_0)/\tau_i}\left(1 - e^{-\Delta t_n/\tau_i}\right) \\ &\quad + \textstyle\sum_{i=1}^N \left(1 - e^{-\Delta t_n/\tau_i}\right)\{\omega_{i,n}\},\end{aligned}$$

where, for the first sum, use was made of the form of $\Delta D_{n,z}$ obtained in Section 5.3 specialized at $z = t_0$. Note that the amplitudes are evaluated at the age of application of the step, $D_i(t_0)$, and that the exponent multiplying the parenthesis is $e^{-(t_{n-1}-t_0)/\tau_i}$, with t_{n-1} (and not t_n), decisive for the consistency verified in Section 6.

With the recurrence for $\{\omega_{i,n}\}$ defined, one finally has:

$$\{\Delta\varepsilon^{cr}_n\} = \{\eta_n\} + q_n\,[\mathbb{V}]\{\Delta\sigma_n\},$$

with

$$q_n = \sum_{i=1}^N D^*_{i,n}\left[1 - \frac{\tau_i}{\Delta t_n}\left(1 - e^{-\Delta t_n/\tau_i}\right)\right].$$

6. Verification: creep test under constant stress

It is now possible to apply the incremental derivation to the simplest case, which is to simulate the creep test itself. The formulation presented must recover exactly the creep function taken as input. Mechanically, creep is the case of a specimen loaded in uniaxial compression at age z_0, applied nearly instantaneously $\Delta\sigma_0 = 1\,\text{MPa}$, and held constant thereafter.

6.1 Reference solution (continuous form)

Setting $t_0 \equiv z_0$ and $\partial\sigma/\partial z = 0$ for $z > z_0$, the equation of Section 4 reduces to its first term:

$$\{\varepsilon^{cr}(t)\} = [\mathbb{V}]\{\Delta\sigma_0\}\, D(t, z_0).$$

Adding the instantaneous elastic part, $[\mathbb{V}]\{\Delta\sigma_0\}/E(z_0)$, the total strain is:

$$\{\varepsilon(t)\} = [\mathbb{V}]\{\Delta\sigma_0\}\left[\frac{1}{E(z_0)} + D(t, z_0)\right] = [\mathbb{V}]\{\Delta\sigma_0\}\, J(t, z_0).$$

Being a uniaxial state, $\{\sigma\} = \{\Delta\sigma_0, 0, 0, 0, 0, 0\}^T$, and with the entry $V_{(1,1)}$ of $[\mathbb{V}]$ equal to 1,

$$\varepsilon_{11}(t) = \Delta\sigma_0\, J(t, z_0) = J(t, z_0) \times 1\,\mathrm{MPa},$$

and in the transverse directions, $\varepsilon_{22} = \varepsilon_{33} = -\nu\,\Delta\sigma_0\, J(t, z_0)$ — that is, transverse creep follows the same elastic Poisson's ratio, consistent with the hypothesis adopted in Section 2. Numerically, with $\Delta\sigma_0 = 1\,\mathrm{MPa}$ and J expressed in $10^{-6}/\mathrm{MPa}$, the axial strain coincides in value with $J(t, z_0)$, which the incremental algorithm must reproduce.

6.2 Path of the incremental algorithm

Discretizing time into arbitrary steps $t_0 < t_1 < ... < t_k$, not necessarily equal, and applying the load as a step, one has $\{\Delta\sigma_n\} = \mathbf{0}$ for every $n \geq 1$. Going through the three terms of the increment:

Part I is proportional to the current increment and therefore vanishes at all steps:

$$q_n\, [\mathbb{V}]\{\Delta\sigma_n\} = \mathbf{0}, \qquad n \geq 1.$$

The auxiliary variables start from $\{\omega_{i,1}\} = \mathbf{0}$ and, by the recurrence, remain null, since the part that updates them is proportional to $\{\Delta\sigma_{n-1}\}$, which is null for $n - 1 \geq 1$:

$$\{\omega_{i,n}\} = \underbrace{[\mathbb{V}]\{\mathbf{0}\}\, D^*_{i,n-1}\frac{\tau_i}{\Delta t_{n-1}}\left(1 - e^{-\Delta t_{n-1}/\tau_i}\right)}_{=\,\mathbf{0}} + \underbrace{\{\omega_{i,n-1}\}}_{=\,\mathbf{0}} e^{-\Delta t_{n-1}/\tau_i} = \mathbf{0}.$$

Hence $II = \mathbf{0}$ at all steps: the initial step is accounted for only by the term $\Delta D_{n,0}$, and the recurrence of the auxiliary variables is not mobilized.

There remains, therefore, only the hereditary term of the step:

$$\{\Delta\varepsilon^{cr}_n\} = \{\eta_n\} = [\mathbb{V}]\{\Delta\sigma_0\}\,\Delta D_{n,0} = [\mathbb{V}]\{\Delta\sigma_0\}\left[D(t_n, z_0) - D(t_{n-1}, z_0)\right].$$

6.3 Sum of increments and recovery of the creep function

Accumulating the increments from $n = 1$ up to a generic instant t_k, the intermediate terms cancel in pairs:

$$\begin{aligned}\{\varepsilon^{cr}(t_k)\} &= \textstyle\sum_{n=1}^{k} \{\Delta\varepsilon^{cr}_n\} = [\mathbb{V}]\{\Delta\sigma_0\}\textstyle\sum_{n=1}^{k}\left[D(t_n, z_0) - D(t_{n-1}, z_0)\right] \\ &= [\mathbb{V}]\{\Delta\sigma_0\}\left[D(t_k, z_0) - D(t_0, z_0)\right].\end{aligned}$$

Since $t_0 = z_0$ and, by the property established in Section 3, $D(z_0, z_0) = 0$, one obtains

$$\{\varepsilon^{cr}(t_k)\} = [\mathbb{V}]\{\Delta\sigma_0\}\, D(t_k, z_0),$$

which is exactly the reference solution of Section 6.1. Adding the elastic part,

$$\varepsilon_{11}(t_k) = \Delta\sigma_0 \, J(t_k, z_0),$$

that is, **the algorithm recovers exactly the creep function itself**.

Three aspects deserve emphasis. First, the coincidence is exact, not approximate: no discretization error is introduced, whatever the sequence $\{\Delta t_n\}$ adopted. This occurs because, in the step term, the amplitudes are evaluated at the exact loading age, $D_i(z_0)$, and not by the mid-point quadrature $D^*_{i,n}$ — the mid-point approximation acts only on the *continuous* part of the history, which is absent in this case. Second, the verification is sensitive to the exponent $e^{-(t_{n-1} - z_0)/\tau_i}$ present in $\{\eta_n\}$, without which the intermediate terms would not cancel so that the result recovers the creep function exactly. Third, in the incremental constitutive equation of Section 2 the elastic modulus is evaluated at the current age; since $\{\Delta\sigma_n\} = \mathbf{0}$ for $n \geq 1$, no further elastic strain is accumulated by the aging of E, only the instantaneous part that remains fixed at $1/E(z_0)$, precisely as required by the definition $J(t, z) = 1/E(z) + D(t, z)$.

6.4 Complementary verification: ramp loading

A second test, useful because it exercises the parts q_n and $\{\omega_{i,n}\}$, consists in applying $\Delta\sigma_1$ as a constant-rate ramp over the first step $[t_0, t_1]$, holding the stress constant thereafter. The exact solution, under the same hypothesis of constant amplitude within the step, is:

$$\varepsilon^{cr}(t) = \Delta\sigma_1 \sum_{i=1}^{N} D^*_{i,1} \left[1 - \frac{\tau_i}{\Delta t_1} \left(1 - e^{-\Delta t_1/\tau_i} \right) e^{-(t - t_1)/\tau_i} \right], \qquad t \geq t_1.$$

At $t = t_1$ the exponential equals 1 and the expression reduces to $q_1 \Delta\sigma_1$, coinciding with the first increment supplied by the algorithm. For $t = t_2$, the difference $\varepsilon^{cr}(t_2) - \varepsilon^{cr}(t_1)$ equals:

$$\Delta\sigma_1 \sum_{i=1}^{N} D^*_{i,1} \frac{\tau_i}{\Delta t_1} \left(1 - e^{-\Delta t_1/\tau_i} \right) \left(1 - e^{-\Delta t_2/\tau_i} \right) = \sum_{i=1}^{N} \left(1 - e^{-\Delta t_2/\tau_i} \right) \{\omega_{i,2}\},$$

with $\{\omega_{i,2}\}$ given by the recurrence of Section 5.3.1, and again the coincidence is exact. As $\Delta t_1 \to 0$ the ramp converges to a simple step and $q_1 \to 0$, recovering the case of Section 6.1. The two ways of introducing the *same* mechanical load — step $\{\Delta\sigma_0\}$ (term in $\Delta D_{n,0}$) or ramp in the first step ($\Delta\sigma_1$ via q_n and $\{\omega_{i,n}\}$) — are therefore consistent with each other. This in no way restricts histories in which temperature varies (including as a ramp) concurrently with the test or with the application of the load: temperature enters through the reduced time ξ and through the part $\boldsymbol{\varepsilon}^{th}$, independently of how the stress jump or ramp is represented.

7. Formulation for finite elements

At the beginning of step n one knows:

- the stress history up to t_{n-1} (in particular $\{\Delta\sigma_{n-1}\}$ and, if any, $\{\Delta\sigma_0\}$);
- the auxiliary variables $\{\omega_{i,n}\}$ updated by the recurrence (or, equivalently, updated *after* step $n-1$);
- the scalar q_n, a function only of Δt_n and of the D_i, τ_i.

Unknown are $\{\Delta\sigma_n\}$ and the total strain increment. The decomposition:

$$\{\Delta\varepsilon^{cr}_n\} = \{\eta_n\} + q_n \, [\mathbb{V}]\{\Delta\sigma_n\}$$

allows treating $\{\eta_n\}$ as a creep strain already determined by the history — in the same sense as the hereditary terms of Zocher et al.'s formulation — and incorporating $q_n[\mathbb{V}]$ into the incremental constitutive operator of the step. Viscoelastic equilibrium with aging reduces, at each step, to a linear elastic problem (or elastic with imposed strains), solved by the finite-element method.

It is not necessary to derive the isoparametric element differently: the assembly of K and the nodal equilibrium are those of linear elasticity theory. Incrementalization alters only the *constitutive operator of the step* and the vector of imposed strains.

Starting from the constitutive equation of Section 2 and from the decomposition $\{\Delta\varepsilon_n^{cr}\} = \{\eta_n\} + q_n[\mathbb{V}]\{\Delta\sigma_n\}$, the stress increment at step n is written, in Voigt form:

$$\{\Delta\sigma_n\} = [\mathbb{C}_n]\Big(\{\Delta\varepsilon_n^{tot}\} - \{\Delta\varepsilon_n^{th}\} - \{\Delta\varepsilon_n^{aut}\} - \{\eta_n\}\Big),$$

where the tangent operator of the step,

$$[\mathbb{C}_n] = \Big(\tfrac{1}{E_n}[\mathbb{V}] + q_n[\mathbb{V}]\Big)^{-1} = \frac{E_n}{1 + q_n E_n}[\mathbb{V}]^{-1},$$

absorbs the part $q_n[\mathbb{V}]$ of creep (with $E_n = E(t_n)$ on the coherent unit scale of q_n). The parts $\{\eta_n\}$, thermal and autogenous, enter as imposed strains known at the beginning of the step and generate the equivalent nodal force vector $F_n^{\eta,\,\mathrm{th}}$. Equilibrium at the step reduces to

$$K_n\, u_n = F_n^{\mathrm{ext}} + F_n^{\eta,\,\mathrm{th}},$$

with K_n assembled from $[\mathbb{C}_n]$. Once $\{\Delta\sigma_n\}$ is obtained, the variables $\{\omega_{i,n+1}\}$ are updated (Section 5.3.1) and one advances to the next step.

7.1 Comparison with Zocher et al. (1997)

The comparison with Zocher, Groves and Allen (1997) highlights three points:

1. **Starting constitutive function.** Those authors start from the *relaxation moduli* (Dirichlet–Prony series on relaxation); in this work, one starts from the *creep function* $D(t, z)$, which is the quantity directly tied to the concrete creep test.
2. **Aging.** In Zocher et al.'s formulation, aging of young concrete is not the object of the representation. Here, by contrast, the dependence of D_i on the loading age z (or ξ') is retained throughout the history.
3. **Same numerical strategy.** In both cases, the constant-rate hypothesis and the analytical evaluation of the integral of the exponential series within the step allow *closing* the integrals and obtaining the recurrence, eliminating full storage of the history.

For mass concrete subject to a temperature history, the route through the creep function with aging obtained by test is a necessary requirement: tests and fitting models (Kelvin chain with aging) supply $J(t, z)$ or $D(\xi, \xi')$; the derivation above converts that information into an incremental algorithm needed for the stress calculation. In short, one shares with Zocher et al. the strategy (elastic problem per step, memory in auxiliary variables), with the difference that $[\mathbb{C}_n]$ and $\{\eta_n\}$ arise from the creep function with aging, and not from a Dirichlet–Prony series on relaxation.

It is worth recording the scope of this same algebraic structure. Souza and Allen (2010) showed that the homogenized incremental viscoelastic constitutive equation of a heterogeneous medium retains the form of the local equation — tangent operator of the step plus a history-dependent stress vector — with the difference that both then depend on the accumulated damage at the lower scale. That is, the pair $[\mathbb{C}_n]$, $\{\eta_n\}$ is not peculiar to creep with aging: it is the form that linear viscoelasticity takes when incrementalized, and it survives homogenization and the evolution of microcracks (Souza, 2009; Souza and Allen, 2011).

7.2 Implementation remarks

1. **Reduced time.** In the presence of variable temperature, the retardation times τ_i and the intervals Δt_n must be interpreted in reduced time ξ, or the coefficients must be re-evaluated with the *shift factor* a_T. The algebraic structure of the derivation remains unchanged.
2. **Evaluation of $D^*_{i,n}$.** Taking the mid-point of the interval is the mid-point rule, whose global convergence is second order in Δt — the error falls by a factor near four at each halving of the step, for smooth stress histories. Even so, small steps are needed at early ages, when $D_i(z)$ varies rapidly and Δt itself is of the order of the variation scale. The initial-step term, not passing through that quadrature, is exact (Section 6.3).
3. **Initialization and initial step.** At $n = 1$, $\{\omega_{i,1}\} = \mathbf{0}$. If there is no jump $\{\Delta\sigma_0\}$ at t_0, the corresponding term in $\{\eta_n\}$ vanishes. The step, when present, is accounted for exclusively by $\Delta D_{n,0}$ and never by the recurrence.
4. **Update order.** At each step, one computes q_n and $\{\eta_n\}$ with $\{\omega_{i,n}\}$ coming from the previous step, solves equilibrium obtaining $\{\Delta\sigma_n\}$, and only then updates $\{\omega_{i,n+1}\}$.
5. **Numerical stability.** For $\Delta t_n \ll \tau_i$, the expressions $1 - e^{-\Delta t_n/\tau_i}$ and $1 - (\tau_i/\Delta t_n)(1 - e^{-\Delta t_n/\tau_i})$ suffer loss of precision by cancellation in floating-point arithmetic; it is advisable to compute $e^x - 1$ by a stable routine for that difference — the routine `expm1`, for example — or by series expansion of the small argument.
6. **Thermal coupling.** The thermal strain $\boldsymbol{\varepsilon}^{th} = \alpha_T \Delta\theta\,\mathbf{1}$ (isotropic) enters the incremental constitutive equation of Section 2; creep acts on the stress history generated by the restraints to that strain (and to the other parts).
7. **Cracking index.** Once the history of principal stresses is obtained, the largest principal stress is compared with the evolution of the tensile strength (a function of maturity). The relation to the classical strain-capacity criterion is discussed in Section 9. This is a verification, not a cracking model: representing the passage from microcracks to a macrocrack in a viscoelastic medium requires a two-scale treatment with two-way coupling (Souza and Allen, 2011), outside the scope of this Part I.

8. Analytical–numerical validation

The analytical–numerical validation based on the formulation presented is set out at two levels: (i) a specialized version *without* aging, in the same sense as the examples of Zocher et al. (1997); (ii) plane stress or plane strain, as applicable, *with* aging, including cyclic loading and a frequency-domain formulation with the resulting application in the time domain. The *free* slab under hydration (non-separable thermal field) is presented in Section 8.3.5; the *restrained* slab with a continuous history — a typical mass-concrete case and often the most critical — and the comparison with the verification criteria are treated in Section 9.2. The numerical–experimental validation will be carried out later, in a separate paper, with the monitoring and modeling campaign of the Log Spillway (VET) at Santo Antônio HPP.

For the checks with aging, the functional form of the Kelvin chain is adopted

$$D(\xi, \xi') = \sum_{i=1}^{N} D_i(\xi') \left[1 - e^{-(\xi - \xi')/\tau_i}\right],$$

with amplitudes that depend on the loading age,

$$D_i(\xi') = a_i + \sum_{j=1}^{M_i} b_{i,j}\, e^{-\xi'/c_{i,j}},$$

in which a_i is the constant part and the pairs $(b_{i,j}, c_{i,j})$ define the M_i aging exponentials of the i-th unit — one, two or more, as the fit requires.

For the concrete of Itumbiara HPP (Andrade et al., 1997), used here as a fitting example, the model $D_0 + D_1 +$ kernel is adopted: two aging parts $D_0(z)$ and $D_1(z)$, each with two exponentials in z, and a common spectrum $(\tau_j,\ \varphi_j)$ of $M = 11$ Kelvin units that reproduces the logarithmic creep kernel in the form adopted in that work (ln base):

$$J(t, z) = D_0(z) + D_1(z) \sum_{j=1}^{M} \varphi_j \left[1 - e^{-(t-z)/\tau_j} \right], \qquad E(z) = \frac{1}{D_0(z)},$$

with

$$D_p(z) = a_p + b_p\, e^{-z/c_p} + d_p\, e^{-z/c_{p2}}, \qquad p = 0,\ 1.$$

Table 1 — Creep model for Itumbiara HPP (Andrade et al., 1997). Parameters in MPa; time in days.

Quantity	Equation	Parameter 1	Parameter 2	R
Modulus	$E(z) = \dfrac{z}{a_E z + b_E}$	$a_E = 3.619 \times 10^{-5}$	$b_E = 7.750 \times 10^{-5}$	0.993
Creep coefficient	$\varphi(z) = \exp\left(A + B/z \right)$	$A = -12.420$	$B = 1.556$	0.945
Creep	$J(t, z) = \dfrac{1}{E(z)} + \varphi(z)\ln(t - z + 1)$	—	—	—

Table 2 — Constants adopted in the Section 8 checks.

Quantity	Value
ν	0.20
α_T (thermal expansion)	$10 \times 10^{-6}\ {}^\circ\mathrm{C}^{-1}$

Table 3 — Aging parts $D_0(z)$ and $D_1(z)$ of the fit $D_0 + D_1 \cdot$ kernel.

Part	a_p (MPa^{-1})	b_p (MPa^{-1})	d_p (MPa^{-1})	c_p (d)	c_{p2} (d)
D_0	3.700×10^{-5}	5.479×10^{-5}	1.110×10^{-5}	2.416	16.063
D_1	2.838×10^{-5}	4.624×10^{-5}	6.117×10^{-6}	2.416	16.063

z (d)	$D_0(z)$ (MPa^{-1})	$D_1(z)$ (MPa^{-1})	$E(z) = 1/D_0$ (MPa)
1	8.365×10^{-5}	6.470×10^{-5}	11 955
3	6.203×10^{-5}	4.682×10^{-5}	16 120
7	4.720×10^{-5}	3.489×10^{-5}	21 187
28	3.894×10^{-5}	2.945×10^{-5}	25 681
91	3.703×10^{-5}	2.840×10^{-5}	27 002

The unit amplitudes are $D_j(z) = \varphi_j\, D_1(z)$, with retardation times τ_j in days. The kernel was discretized with $L_{\ln} = 3.000$ decades in τ ($\tau_1/\tau_M \approx 2.0 \times 10^{-4}$).

Table 4 — Logarithmic-kernel spectrum: $M = 11$ Kelvin units.

j	τ_j (d)	φ_j
1	0.3099	5.299×10^{-3}
2	0.7619	3.488×10^{-2}
3	1.8729	7.646×10^{-2}
4	4.6040	1.047×10^{-1}
5	11.318	1.193×10^{-1}
6	27.821	1.255×10^{-1}
7	68.390	1.286×10^{-1}
8	168.12	1.280×10^{-1}
9	413.27	1.401×10^{-1}
10	1015.9	6.710×10^{-2}
11	2497.3	3.274×10^{-1}

The chain fit to the $J(t, z)$ curves of the predictor model reproduces the kernel with a median relative error of 9.7×10^{-6} and $R^2 = 0.999995$. In this section what matters is the form of the equations and the check that the algorithm based on $\{\eta_n\}$, q_n reproduces reference solutions with this model. The relaxation modulus R, when needed, was obtained from J by Bažant's recurrence (1972) in the form of Sassone and Chiorino (2005) or by the $\{\eta_n\}$, q_n algorithm itself.

8.1 Particular case without aging (Zocher et al. type, 1997)

When D_i and E are independent of loading age, the formulation in this paper reduces to classical linear viscoelasticity, starting from creep rather than relaxation. The standard linear solid (SLS), material A, of Zocher, Groves and Allen (1997) is adopted,

$$R(t) = E_\infty + (E_0 - E_\infty)\, e^{-t/\tau_\sigma}, \qquad J(t) = \frac{1}{E_0} + \left(\frac{1}{E_\infty} - \frac{1}{E_0}\right)\left(1 - e^{-t/\tau_\varepsilon}\right),$$

with $\tau_\varepsilon = \tau_\sigma E_0/E_\infty$, $E_0 = 0.5\,\mathrm{MPa}$, $E_\infty = 0.1\,\mathrm{MPa}$, $\tau_\sigma = 1$ t.u. and $\nu = 0.3$. In all cases below the analytical solution (correspondence principle, with $1/E \to J(t)$) is compared with the numerical response in which $J(t)$ is obtained by the $\{\eta_n\}$, q_n algorithm under unit stress. Example 3 of Zocher et al. (orthotropic cylinder) is not reproduced.

Cantilever beam with tip load (Zocher, Ex. 1). With $P(t) = P_0\left[H(t) - H(t - t_1)\right]$,

$$w_L(t) = \frac{P_0 L^3}{3I}\left[J(t) - J(t - t_1)\, H(t - t_1)\right].$$

Thick cylinder encased in a rigid shell (Zocher, Ex. 2). Internal pressure $p_0 H(t)$, $u_r(b) = 0$:

$$u_r(r, t) = p_0\, \frac{a^2 b\,(1 + \nu)(1 - 2\nu)}{a^2 + (1 - 2\nu) b^2}\left(\frac{b}{r} - \frac{r}{b}\right) J(t).$$

Classical thin ring. Mean radius a, thickness $h \ll a$, internal pressure $p_0 H(t)$, plane stress ($\sigma_\theta = p_0 a/h$, $\sigma_r \approx 0$):

$$u_r(t) = \frac{p_0 a^2}{h}\, J(t).$$

Infinite plate with a circular hole (Kirsch). Remote tension $\sigma_\infty H(t)$ in plane stress; with ν constant the stresses coincide with the elastic ones and, at the hole edge,

$$u_r(a,t) = 3a\sigma_\infty\, J(t).$$

The layouts of the four cases are in Figure 2; the geometric and loading parameters, in Table 5; the responses, in Figure 3. In addition, with the same SLS family at concrete scale ($E_0 = 25\,\mathrm{GPa}$, $E_\infty = 5\,\mathrm{GPa}$), Figure 1 presents two comparisons: (i) analytical R with R obtained via J (Bažant recurrence), with the curves overlapping as functions of $t - z$ — no aging; (ii) in plane stress with ΔT, the stress via R with the incremental formulation η_n, q_n.

Table 5 — Parameters of the isotropic benchmarks without aging. Length units in metres; time in the unit of the Zocher et al. (1997) examples.

	Beam (Ex. 1)	Fixed cylinder (Ex. 2)	Thin ring	Plate with hole
Material	A (SLS)	A (SLS)	A (SLS)	A (SLS)
E_0 (MPa)	0.5	0.5	0.5	0.5
E_∞ (MPa)	0.1	0.1	0.1	0.1
τ_σ (t.u.)	1	1	1	1
ν	0.3	0.3	0.3	0.3
Geometry	$L = 20$, $I = 1/12$	$a = 2$, $b = 4$, $r = (a+b)/2$	$a = 1$, $h = 0.05$	$a = 1$
Loading	$P_0 = 1$, $t_1 = 10$	$p_0 = 100\,\mathrm{Pa}$	$p_0 = 0.01\,\mathrm{MPa}$	$\sigma_\infty = 0.01\,\mathrm{MPa}$
Response	$w_L(t)$	$u_r(r,t)$	$u_r(t)$	$u_r(a,t)$

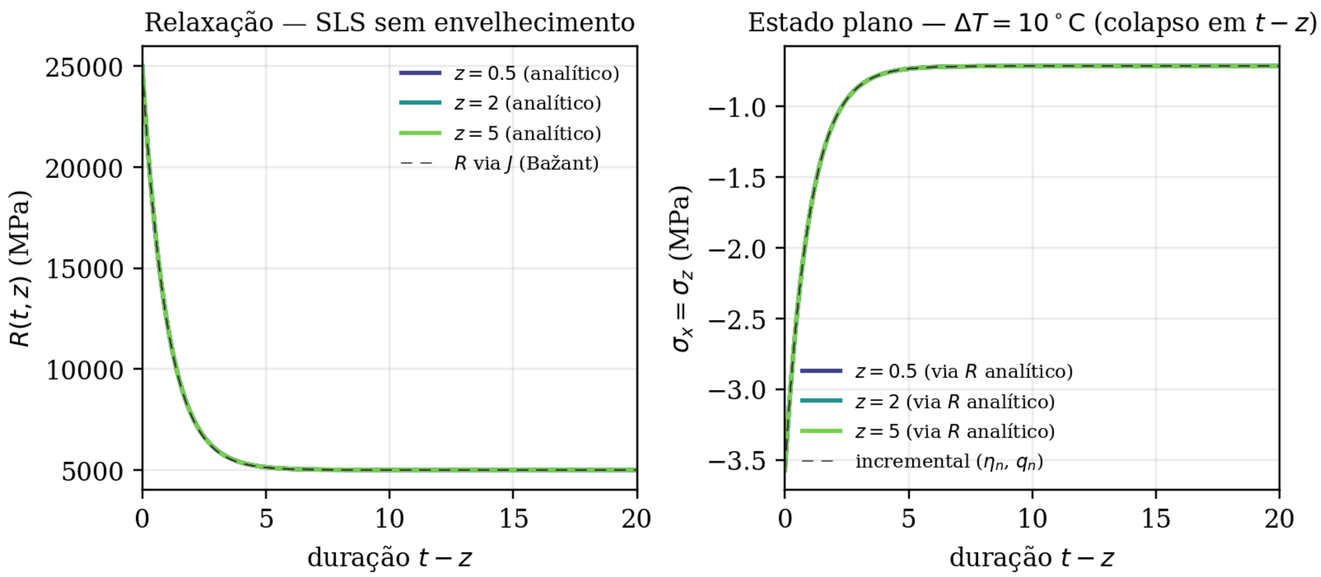

Figure 1 — Without aging (SLS, Zocher ratios, concrete scale): $R(t - z)$ and plane stress with $\Delta T = 10^\circ\mathrm{C}$ — overlapping curves in $t - z$; dashed: incremental.

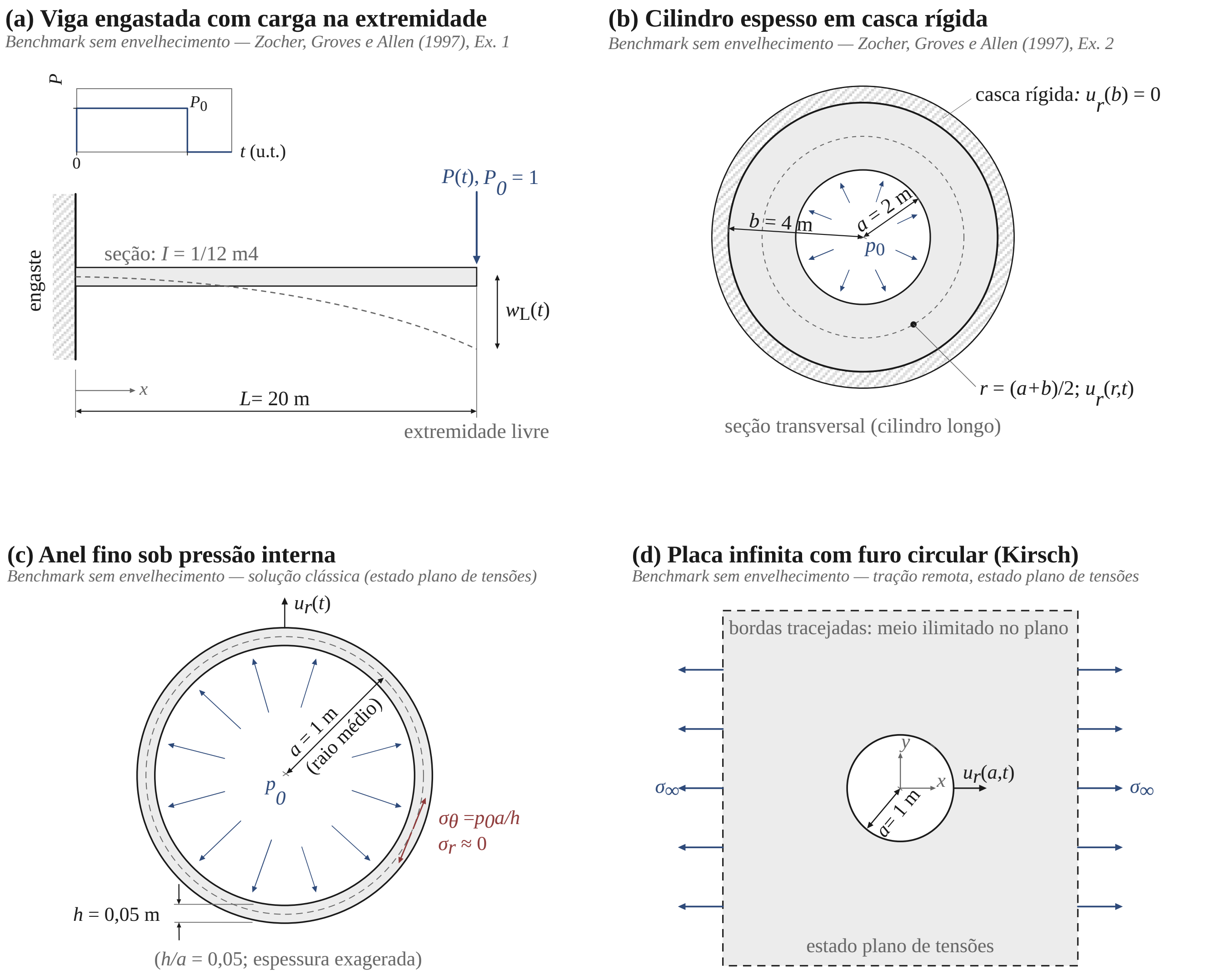

Figure 2 — Layouts of the isotropic benchmarks without aging (material A): (a) beam; (b) fixed cylinder; (c) thin ring; (d) plate with hole.

(a) Beam. Geometry: $L = 20\,\mathrm{m}$; $I = 1/12\,\mathrm{m}^4$ (unit cross-section). Boundary: fixed at $x = 0$ ($w = w' = 0$); end $x = L$ free. Loading: $P(t) = P_0\left[H(t) - H(t - t_1)\right]$, $P_0 = 1$, $t_1 = 10$. Material: A (SLS): $E_0 = 0.5\,\mathrm{MPa}$, $E_\infty = 0.1\,\mathrm{MPa}$, $\tau_\sigma = 1\,\mathrm{t.u.}$, $\nu = 0.3$. Response: $w_L(t) = (P_0 L^3/3I)\left[J(t) - J(t - t_1)H(t - t_1)\right]$.

(b) Fixed cylinder. Geometry: inner radius $a = 2\,\mathrm{m}$; outer radius $b = 4\,\mathrm{m}$; $r = (a + b)/2 = 3\,\mathrm{m}$ (reading point). Boundary: $\sigma_r(a) = -p_0 H(t)$; $u_r(b) = 0$ (rigid shell). Loading: internal pressure $p_0 = 100\,\mathrm{Pa}$, applied as a step at $t = 0$ and held. Material: A (SLS), same parameters as (a). Response: $u_r(r, t) = p_0 \dfrac{a^2 b(1 + \nu)(1 - 2\nu)}{a^2 + (1 - 2\nu)b^2} \left(\dfrac{b}{r} - \dfrac{r}{b} \right) J(t)$.

(c) Thin ring. Geometry: mean radius $a = 1\,\mathrm{m}$; thickness $h = 0.05\,\mathrm{m}$ $(h/a = 0.05)$. Boundary: internal pressure $p_0 H(t)$ on the inner face; outer face free; plane stress. Loading: $p_0 = 0.01\,\mathrm{MPa}$, as a step at $t = 0$ and held. Material: A (SLS), same parameters as (a). Response: $\sigma_\theta = p_0 a/h$ (constant); $u_r(t) = (p_0 a^2/h)\, J(t)$.

(d) Plate with hole. Geometry: infinite plate in the plane, circular hole of radius $a = 1\,\mathrm{m}$. Boundary: hole edge free $(\sigma_r = \tau_{r\theta} = 0$ at $r = a)$; uniform tension σ_∞ at infinity. Loading: $\sigma_\infty H(t)$, $\sigma_\infty = 0.01\,\mathrm{MPa}$, as a step at $t = 0$ and held. Material: A (SLS), same parameters as (a). Response: stresses equal to the elastic ones (ν constant); $u_r(a, t) = 3a\sigma_\infty\, J(t)$.

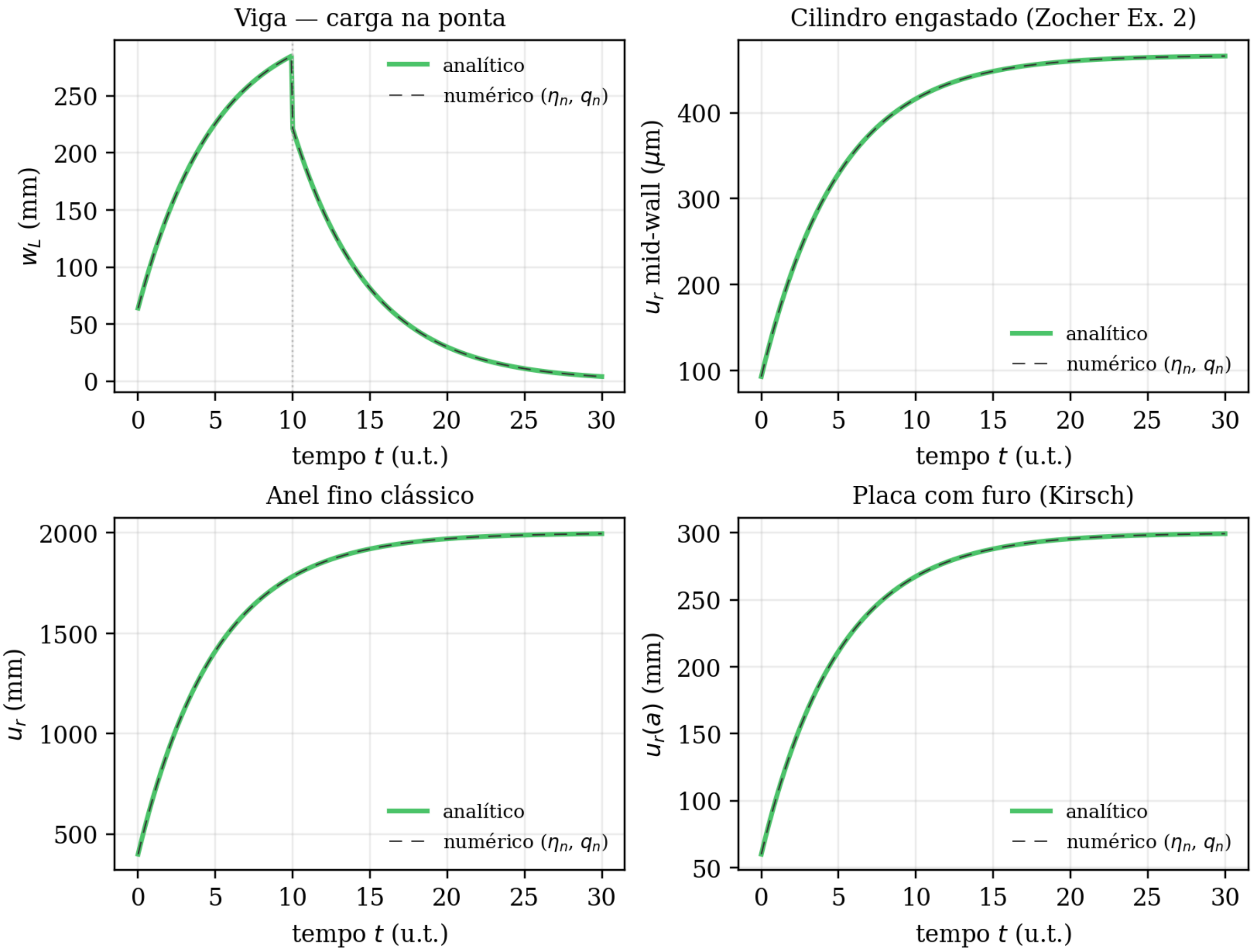

Figure 3 — Isotropic benchmarks without aging (material A): beam; fixed cylinder; thin ring; plate with hole. Solid: analytical correspondence; dashed: J via η_n, q_n.

8.2 Plane strain with uniform ΔT (with aging)

In this classical problem, the element undergoes a uniform temperature change ΔT in time, with displacements prevented in x and z and free in y. The viscoelastic solution corresponding to the elastic solution with the elastic modulus replaced by the relaxation modulus (Zhu, 2014) is:

$$\sigma_x = \sigma_z = -R(t,z)\,\frac{\alpha_T \Delta T}{1-\nu}, \qquad \varepsilon_y = (1+\nu)\,\frac{\alpha_T \Delta T}{1-\nu},$$

in which z is the age at which the thermal step is applied and $R(t,z)$ is the uniaxial relaxation modulus. The expression above is the *analytical* response of the problem, from the elastic–viscoelastic correspondence principle, once R is known; it requires the numerical evaluation of R from creep.

8.2.1 Relaxation from creep (Bažant; Sassone and Chiorino)

The relaxation modulus $R(t,z)$ and the creep compliance $J(t,z)$ are not each the algebraic inverse of the other. As when there is no aging, R is obtained by numerical integration of the integral identity that links the two functions, in the form of Bažant's recurrence (1972), as revisited and presented by Sassone and Chiorino (2005). In essence, a unit strain step is imposed at age z and the stress history $\sigma(t) = R(t,z)$ compatible with

$$\varepsilon(t_n) = \sum_{j=0}^{n} J(t_n, t_j)\,\Delta\sigma_j = 1 \quad (t_n \ge z),$$

is solved step by step, isolating $\Delta\sigma_n$ at each mesh instant. Figures 4 and 5 result from that recurrence, applied to the same $J = 1/E + D$ of the Kelvin chain with aging. Because, with aging, there is no analytical interconversion between J and R, the thermodynamic constraints admissible for the material can only be imposed by the choice of the J family; the resulting relaxation modulus is a numerical consequence of that choice, and not the object of a second independent fit.

8.2.2 Comparison with the incremental algorithm

With $R(t, z)$ available, the restrained stress $\sigma_x = \sigma_z$ follows from the analytical expression above. In parallel, the same history is integrated by the algorithm $\{\Delta\varepsilon_n^{cr}\} = \{\eta_n\} + q_n[\mathbb{V}]\{\Delta\sigma_n\}$ of Sections 4–5, imposing constant mechanical strain after the thermal step (relaxation under restraint). The comparison is made for $\Delta T = 10^\circ\mathrm{C}$ applied at ages $z = 1$, 3, 7, 28 and 91 days, with the age scale from $t = 0$. In all cases, the analytical curve (via R) and the incremental one $(\eta_n,\ q_n)$ coincide within the discretization limit, evidence of correct implementation also with aging.

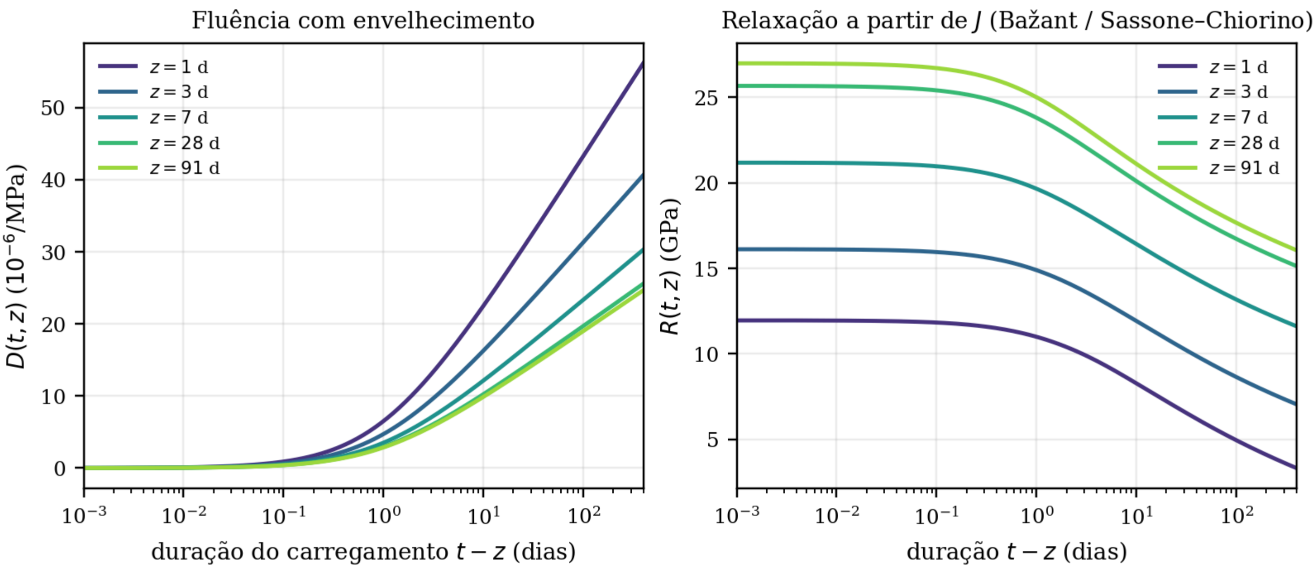

Figure 4 — Creep with aging $D(t, z)$ and relaxation modulus $R(t, z)$ for loading ages $z = 1$, 3, 7, 28 and 91 days.

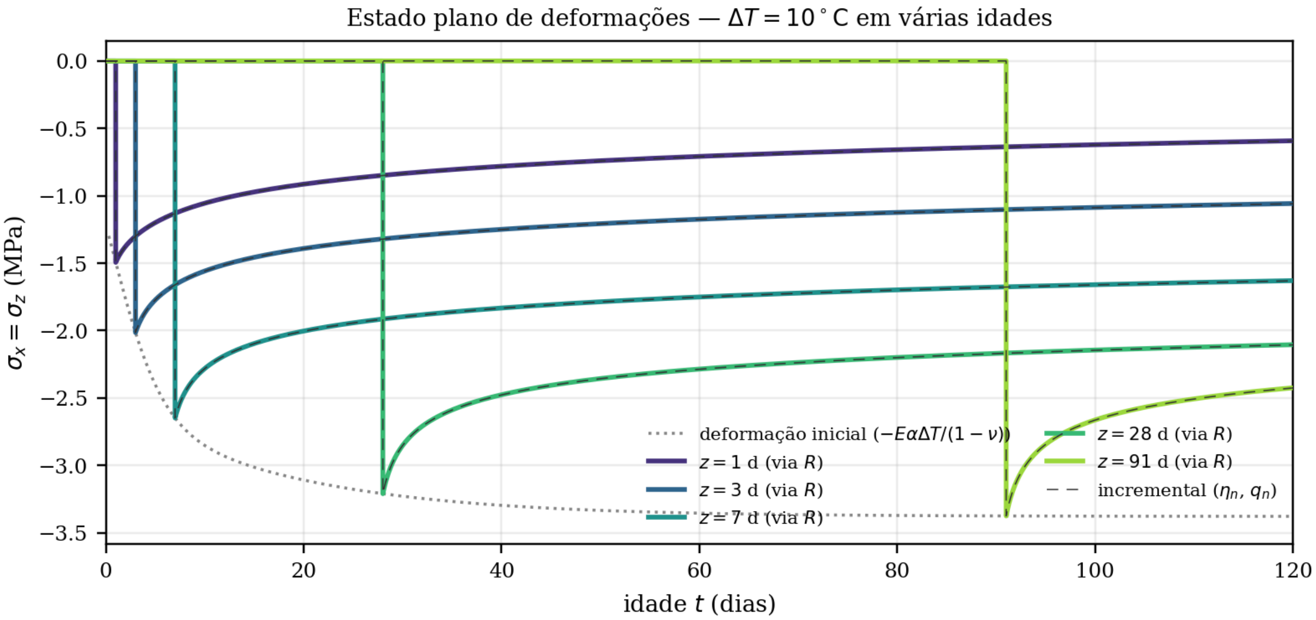

Figure 5 — Plane strain with $\Delta T = 10^\circ\mathrm{C}$ at several ages z: calculation via R and incremental formulation η_n, q_n;
stress from the initial strain $-E(t)\,\alpha_T \Delta T/(1-\nu)$ (dotted).

8.3 Fields with known thermoelastic solution

The cases of Sections 8.1 and 8.2 are one-dimensional problems varying in time. It is also of interest to check the procedure on 2D and 3D fields, that is, on problems in which the stress varies from point to point. There is a family of thermoelastic problems in which this can be done without integrating the entire structure, and it is useful to delimit it before presenting the cases.

Separability condition. Consider a homogeneous body, with constant elastic ν, whose temperature, measured from the stress-free state at instant t_0, is written in the form

$$T(x,t) = \theta(t)\, h(x),$$

with h fixed in space. The corresponding thermoelastic stress is

$$\sigma^e_{ij}(x,t) = \frac{\alpha_T E}{1-\nu}\,\theta(t)\, g_{ij}(x),$$

in which g_{ij} depends only on the geometry, on h and on ν, and not on the elastic modulus. Under that condition, the stress history at each point is proportional to the same function of time, and the viscoelastic problem with aging reduces to a single scalar hereditary problem:

$$\sigma_{ij}(x,t) = g_{ij}(x)\, S(t),$$

with S obtained from the restrained strain $\varepsilon^*(t) = \alpha_T\theta(t)/(1-\nu)$. It is the same application of Zhu's proportional-deformation structures (Section 9.3): once the spatial form is fixed, the viscoelastic response is obtained from the elastic response without point-by-point integration.

Two observations delimit the scope of the solution. The first is that the condition falls on the *form* of T, not on its amplitude: if the hydration field varying with the point is considered (with the $T(t)$ history of each point), they do not belong to this family and are treated in Section 8.3.5. The second is that the independence of g_{ij} with respect to E requires homogeneous material; two concretes of distinct stiffnesses, or foundation plus concrete as a set, also do not belong to this family.

8.3.1 Verification with evaluation of g_{ij}

Four fields were adopted, all with closed-form thermoelastic solution; in the first two, h is the fundamental mode of the heat equation (spatial form that decays without changing shape, with λ fixed by the geometry itself). The thermal solution corresponds to the 'fixed-form' hypothesis. For the long solid cylinder of radius b, with $h(r) = J_0(\mu_1 r/b)$ and μ_1 the first root of J_0, the expressions of Timoshenko and Goodier (1970, §151) hold:

$$g_r = \frac{1}{b^2}\int_0^b h\, r\, \mathrm{d}r - \frac{1}{r^2}\int_0^r h\, r\, \mathrm{d}r, \quad g_\theta = \frac{1}{b^2}\int_0^b h\, r\, \mathrm{d}r + \frac{1}{r^2}\int_0^r h\, r\, \mathrm{d}r - h, \quad g_z = \frac{2}{b^2}\int_0^b h\, r\, \mathrm{d}r - h.$$

For the solid sphere, with $h(r) = \mathrm{sinc}(\pi r/b)$, the corresponding expressions are those of Timoshenko and Goodier (1970, §152). The third field is the hollow cylinder in steady state, $h(r) = \ln(b/r)/\ln(b/a)$, which is the case of the cooling pipe and of the tunnel lining; it has closed form,

$$g_\theta = \frac{1}{2\ln(b/a)}\left[1 - \ln\frac{b}{r} - \frac{a^2}{b^2-a^2}\left(1+\frac{b^2}{r^2}\right)\ln\frac{b}{a}\right],$$

with g_r obtained by replacing the term 1 by zero and $(1+b^2/r^2)$ by $(1-b^2/r^2)$. The fourth is the spherical inclusion of radius a with uniform ΔT in an infinite medium of the same material, which represents the lift cast against older concrete: inside, the state is hydrostatic with $g_r = g_\theta = g_\varphi = -2/3$; outside, $g_r = -\frac{2}{3}(a/r)^3$ and $g_\theta = g_\varphi = \frac{1}{3}(a/r)^3$.

The maps were checked before use, each by the resource the case itself offers. For the cylinder and the sphere the boundary and equilibrium conditions were confirmed, $\sigma_r(b) = 0$ and null resultant of σ_z on the cross-section. For the hollow cylinder, numerical integration of the general expressions was compared with the closed form above, with relative deviation of 5×10^{-8}. For the inclusion, the values inside and outside coincide with the classical solution. The layouts of the four cases are in Figure 6; Figure 7 gathers the four spatial kernels g_{ij}; the viscoelastic validation with contour maps is in Figure 8.

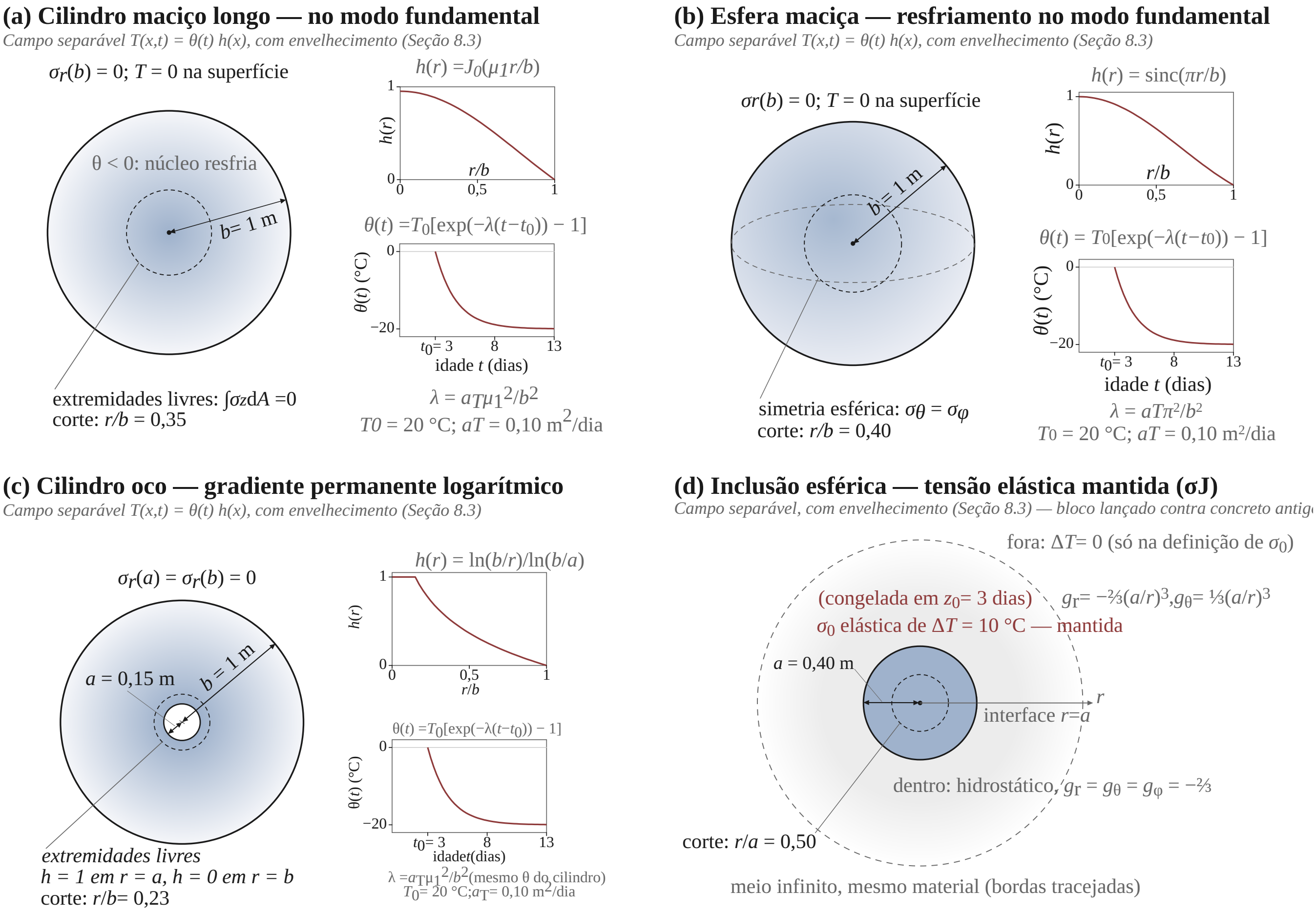

Figure 6 — Layouts of the four separable fields: (a) solid cylinder; (b) solid sphere; (c) hollow cylinder; (d) spherical inclusion.

(a) Solid cylinder. Geometry: long solid cylinder of radius $b = 1\,\mathrm{m}$ (cross-section); reading cut at $r/b = 0.35$. Boundary: free surface, $\sigma_r(b) = 0$; null axial resultant, $\int \sigma_z \,\mathrm{d}A = 0$; $T = 0$ at the surface (reference t_0). Initial cond.: stress-free state at $t_0 = 3$ days; $T(r,t) = \theta(t)\,h(r)$, $\theta(t) = T_0[\exp(-\lambda(t-t_0)) - 1]$, $T_0 = 20\,^\circ\mathrm{C}$. Material: $\nu = 0.20$; $\alpha_T = 10 \times 10^{-6}\,^\circ\mathrm{C}^{-1}$; $E(z)$ and $D(t,z)$ of the Kelvin chain with aging (Itumbiara HPP). Response: $\sigma_\theta(r,t) = g_\theta(r)\,S(t)$, with S obtained from $\varepsilon^*(t) = \alpha_T\theta(t)/(1-\nu)$ by the incremental algorithm.

(b) Solid sphere. Geometry: solid sphere of radius $b = 1\,\mathrm{m}$; reading cut at $r/b = 0.40$. Boundary: free surface, $\sigma_r(b) = 0$; $T = 0$ at the surface (reference t_0). Initial cond.: stress-free state at $t_0 = 3$ days; $T(r,t) = \theta(t)\,h(r)$, $\theta(t) = T_0[\exp(-\lambda(t-t_0)) - 1]$, $T_0 = 20\,^\circ\mathrm{C}$. Material: $\nu = 0.20$; $\alpha_T = 10 \times 10^{-6}\,^\circ\mathrm{C}^{-1}$; $E(z)$ and $D(t,z)$ of the Kelvin chain with aging (Itumbiara HPP). Response: $\sigma_\theta(r,t) = g_\theta(r)\,S(t)$ (Timoshenko and Goodier, §152), S by the incremental algorithm.

(c) Hollow cylinder. Geometry: long hollow cylinder, $a = 0.15\,\text{m}$, $b = 1\,\text{m}$ (cooling pipe, tunnel); cut at $r/b = 0.23$. Boundary: inner and outer faces free, $\sigma_r(a) = \sigma_r(b) = 0$; ends free. Initial cond.: stress-free at $t_0 = 3$ days; $h(r) = \ln(b/r)/\ln(b/a)$ steady, with the same $\theta(t)$ as the solid cylinder. Material: $\nu = 0.20$; $\alpha_T = 10\times10^{-6}\,{}^\circ\text{C}^{-1}$; $E(z)$ and $D(t,z)$ of the Kelvin chain with aging (Itumbiara HPP). Response: $\sigma_\theta(r,t) = g_\theta(r)\,S(t)$, g_θ in closed form (Section 8.3.2); maximum tension at the inner wall.

(d) Spherical inclusion. Geometry: spherical inclusion of radius $a = 0.40\,\text{m}$ in an infinite medium of the same material; cut at $r/a = 0.50$. Boundary: continuity of u_r and σ_r at the interface $r = a$; null stresses at infinity. Loading: at $z_0 = 3$ days the elastic σ of $\Delta T = 10\,{}^\circ\text{C}$ in the sphere is frozen ($\Delta T = 0$ outside) and σ is held. Material: $\nu = 0.20$; $\alpha_T = 10\times10^{-6}\,{}^\circ\text{C}^{-1}$; $E(z)$ and $D(t,z)$ of the Kelvin chain with aging (Itumbiara HPP). Response: σ constant; $\varepsilon_\theta(r,t) = \sigma_\theta(r)\,J(t,z_0)$.

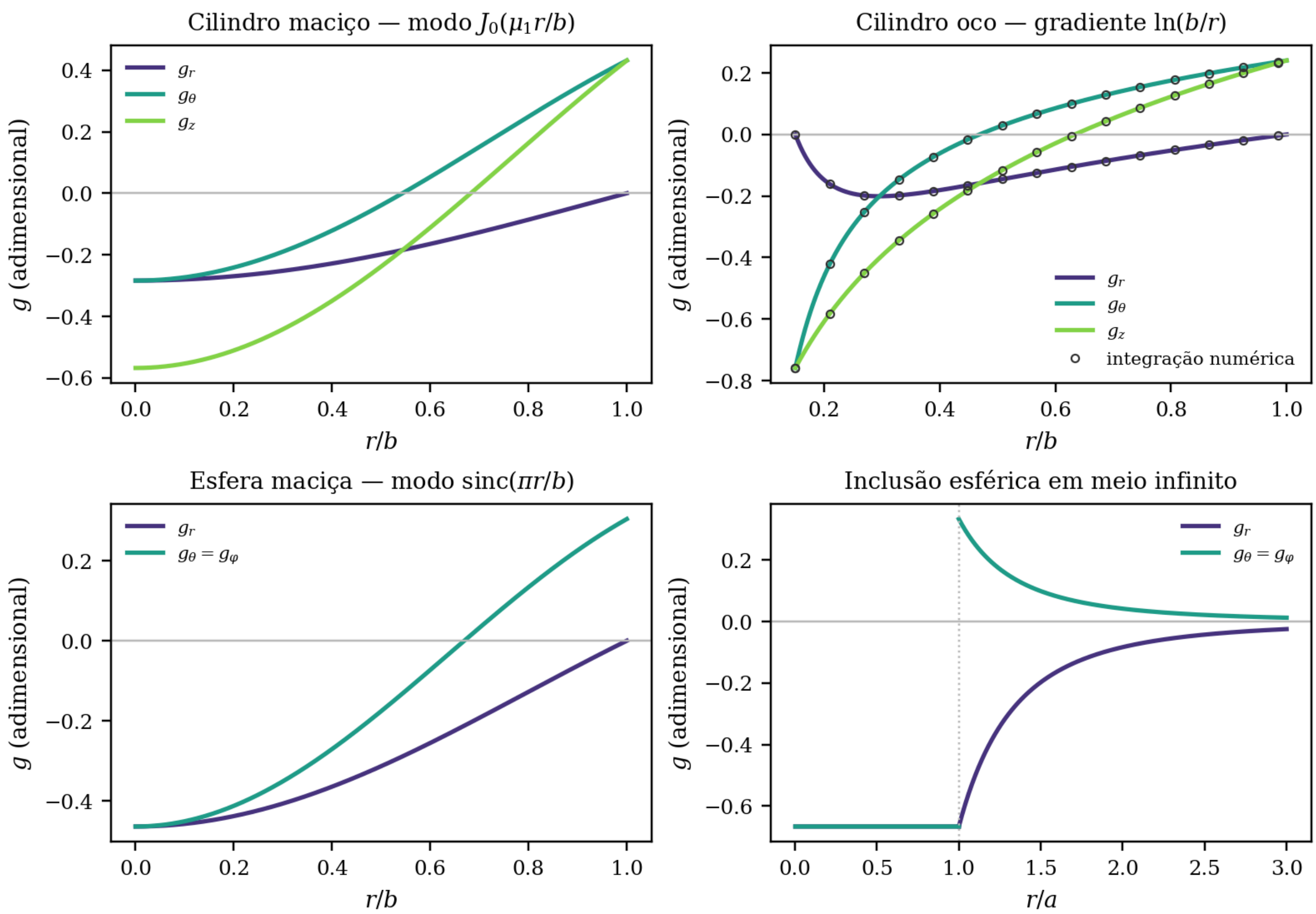

Figure 7 — Maps g_{ij} of the four separable fields: solid cylinder and solid sphere in the fundamental mode, hollow cylinder in steady state and spherical inclusion in an infinite medium. In the hollow cylinder, the markers are the numerical integration of the general expressions over the closed form.

8.3.2 Validation with contour maps

Figure 8 answers a question distinct from Figure 7. The g_{ij} maps confirm the elastic geometry; here one checks whether the incremental algorithm $(\eta_n,\ q_n)$ reproduces, at each point and instant, the viscoelastic response with aging when the thermal field is separable. In terms of Section 8.3.1, the mechanical strain $\varepsilon^*(t) = \alpha_T\theta(t)/(1-\nu)$ is imposed — the counterpart of replacing E by R in the restrained problem — and $S(t)$ obtained by the hereditary integral is compared with the same factor computed incrementally; the full field is $\sigma_{ij} = g_{ij}\,S(t)$. In the fourth panel the question is different: the elastic stress of z_0 is frozen (stress control) and the strain is left to grow with $J(t,z_0)$ — a test that recovers J in a triaxial state, distinct from the relaxation that would follow if the thermal step were held.

The four geometries are those of Section 8.3.2, with scale $b = 1\,\text{m}$. The long solid cylinder and the solid sphere have an external surface free of stress, $\sigma_r(b) = 0$, and null resultant of σ_z on the cross-section; the radial profile $h(r)$ is the fundamental mode of the heat equation, with $T = 0$ at the surface relative to the reference instant. The hollow cylinder has inner radius $a = 0.15\,\text{m}$, free ends and steady profile $h(r) = \ln(b/r)/\ln(b/a)$. The spherical inclusion has radius $a = 0.40\,\text{m}$ in an infinite medium of the same material.

In the first three cases, a stress-free initial state is adopted at $t_0 = 3$ days and cooling $\theta(t) = T_0[\exp(-\lambda(t - t_0)) - 1]$, with $T_0 = 20^\circ\text{C}$ and λ fixed by the diffusivity $h^2 = 0.10\,\text{m}^2/\text{day}$ and by the thermal mode of each body ($\lambda = h^2\mu_1^2/b^2$ in the cylinder, $\lambda = h^2\pi^2/b^2$ in the sphere; in the hollow cylinder, the same $\theta(t)$ is used with steady $h(r)$). In the inclusion, at age $z_0 = 3$ days, the elastic stress corresponding to $\Delta T = 10^\circ\text{C}$ in the sphere is frozen and that stress is held (stress control, not the thermal step). The material is the Kelvin chain with aging of Section 8.2 ($\nu = 0.20$, $\alpha_T = 10 \times 10^{-6}\,{}^\circ\text{C}^{-1}$, $E(z)$ and $D(t, z)$ of Itumbiara HPP).

In each panel, the colour map brings $\sigma_\theta(r, t)$ computed by the incremental algorithm (MPa) in the three thermal cases, or $\varepsilon_\theta(r, t)$ (10^{-6}) in the inclusion; the vertical axis is the normalized radial coordinate (r/b or r/a), the horizontal is age t on a logarithmic scale. The white dashed line indicates the cut radius; below, the profile compares the hereditary reference (solid) and the incremental one (dashed). The maximum relative deviation remains at 10^{-3} in the three stress fields and at 10^{-15} in the inclusion strain.

In the solid cylinder, the core cools and goes into tension; the curve $\sigma_\theta = 0$ remains fixed at $r/b \simeq 0.55$ — a signature of separability. In the sphere, the radial pattern is distinct, but the same logic applies. In the hollow cylinder, tension concentrates at the inner wall. In the inclusion, the dotted line marks the interface $r = a$; on the cut $r/a = 0.50$, ε_θ grows with $J(t, z_0)$ under held stress.

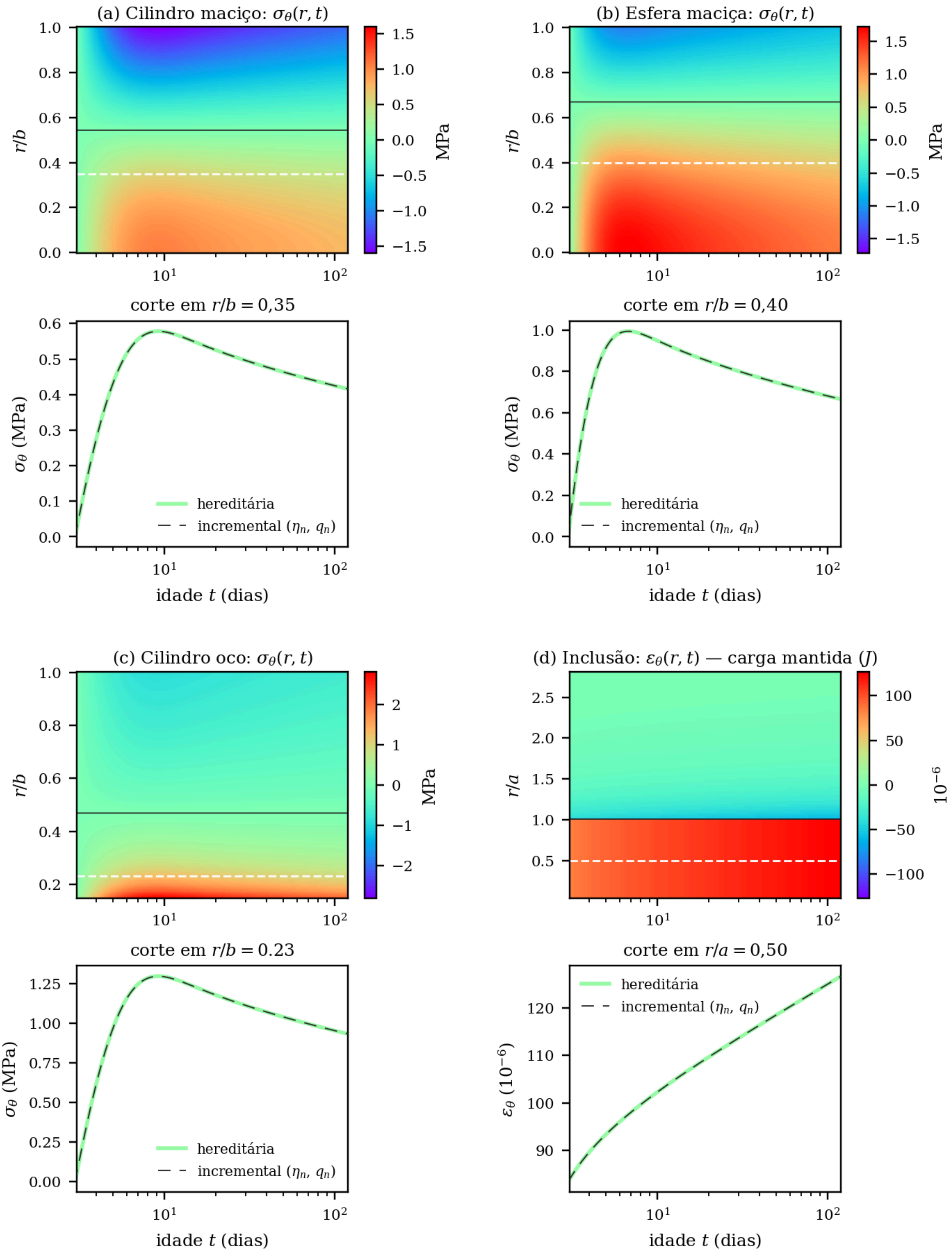

Figure 8 — Viscoelastic validation of the four separable fields ($b = 1$ m, material of Section 8.2). Maps: incremental $\sigma_\theta(r,t)$ in the three cases with cooling from $t_0 = 3$ days; $\varepsilon_\theta(r,t)$ in the inclusion under held elastic stress of $z_0 = 3$ days (σJ). Profiles on the dashed cut: hereditary reference or $\sigma J \times$ algorithm (η_n, q_n).

8.3.3 Cylinder torsion — mechanical loading

Outside the separable family $g_{ij}S(t)$, the first complementary test is purely mechanical, with no temperature change ($\Delta T = 0$). A cylinder of outer radius $R = 0.5\,\mathrm{m}$ and the material of Section 8.2 are adopted. The test traverses the shear diagonal of $[\mathbb{V}]$, absent in the four thermal benchmarks, and safeguards the assembly of the Part II rosette.

Case 1 — held twist. A constant ϕ/L is imposed from $z_0 = 3$ days. The reference is $\tau(r,t) = r(\phi/L)R(t,z_0)/[2(1+\nu)]$. Figure 9 brings the cuts at $r = R$ and $r = 0.25\,\mathrm{m}$ and the map $\tau(r,t)$. The algorithm reproduces the reference with a difference of 8.6×10^{-4} on both cuts.

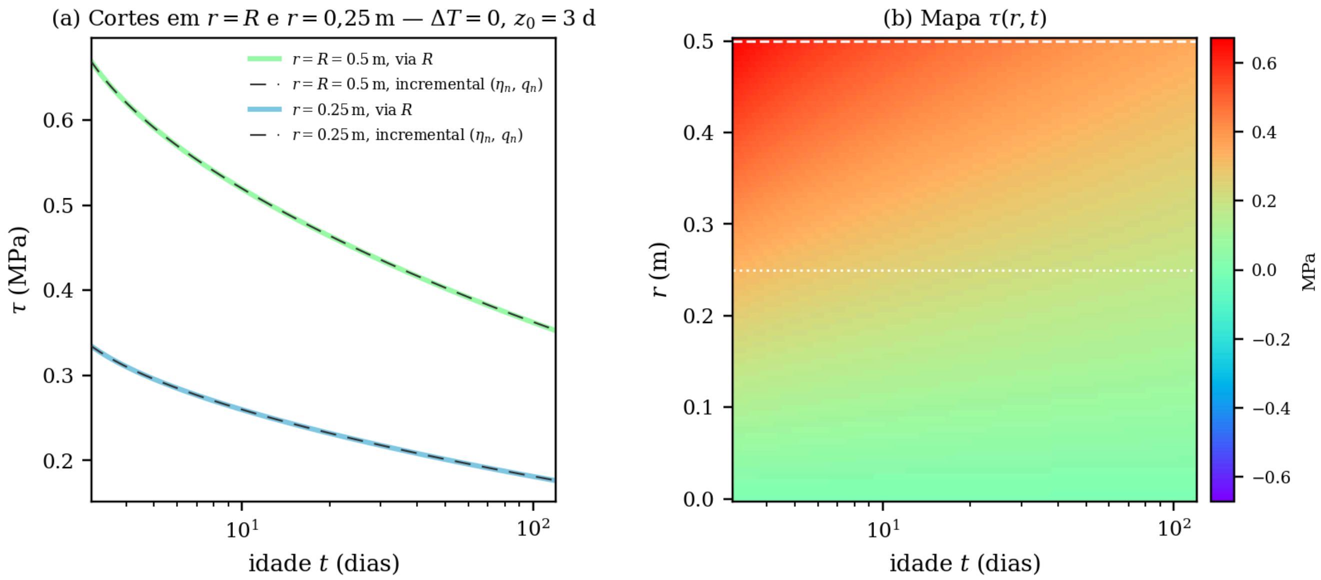

Figure 9 — Cylinder torsion, Case 1 ($R = 0.5\,\mathrm{m}$, $\Delta T = 0$, $z_0 = 3$ d): (a) $\tau(t)$ cuts at $r = R$ and $r = 0.25\,\mathrm{m}$; (b) map $\tau(r,t)$.

Case 2 — harmonic twist. R, ϕ_0/L and the material are kept. The loading imposes, from age z_0,

$$\frac{\phi(t)}{L} = \frac{\phi_0}{L}\left[1 + \kappa \sin\omega(t - z_0)\right], \qquad \kappa = 0.25, \quad \omega = 2\pi\,\mathrm{rad/d}\ (T = 1\,\mathrm{d}),$$

run at $z_0 = 3$ days (same age as Case 1) and at $z_0 = 28$ days. With $J^*(\omega,z) = J'(\omega,z) - iJ''(\omega,z)$ of the Kelvin chain,

$$J'(\omega,z) = \frac{1}{E(z)} + \sum_{i=1}^{N} \frac{D_i(z)}{1 + \omega^2\tau_i^2}, \qquad J''(\omega,z) = \sum_{i=1}^{N} \frac{D_i(z)\,\omega\tau_i}{1 + \omega^2\tau_i^2},$$

and $G^*(\omega,z) = 1/[2(1+\nu)J^*]$, the quasi-stationary reference is written

$$\tau(r,t) = r\frac{\phi_0}{L}\frac{R(t,z_0)}{2(1+\nu)} + r\frac{\phi_0}{L}\kappa\left[G'(\omega,t)\sin\omega(t - z_0) + G''(\omega,t)\cos\omega(t - z_0)\right],$$

with G' and G'' evaluated at the current age t, and not frozen at z_0. Figure 10 brings, for each age, the last five cycles at $r = R$ and the map $\tau(r,t)$. The amplitude and phase of the incremental history are extracted by synchronous detection with drift rejection — the mean part relaxes via $R(t,z_0)$ and is not constant in the window — and compared with $|G^*|$ and δ at the centre of the reading window. The Struik number $S = T/z$ in that window is also reported. At $z_0 = 28$ days ($S = 0.025$),

$e_A = -3.7 \times 10^{-5}$ and $e_\phi = 0.013°$; at $z_0 = 3$ days ($S = 0.069$), $e_A = -7.8 \times 10^{-4}$ and $e_\phi = 0.044°$. The incremental algorithm and the quasi-stationary reference remain superimposed; the cyclic test exposes phase deviation and temporal accumulation in the integration of $\omega_{i,n}$ that Case 1, monotonic, does not reveal.

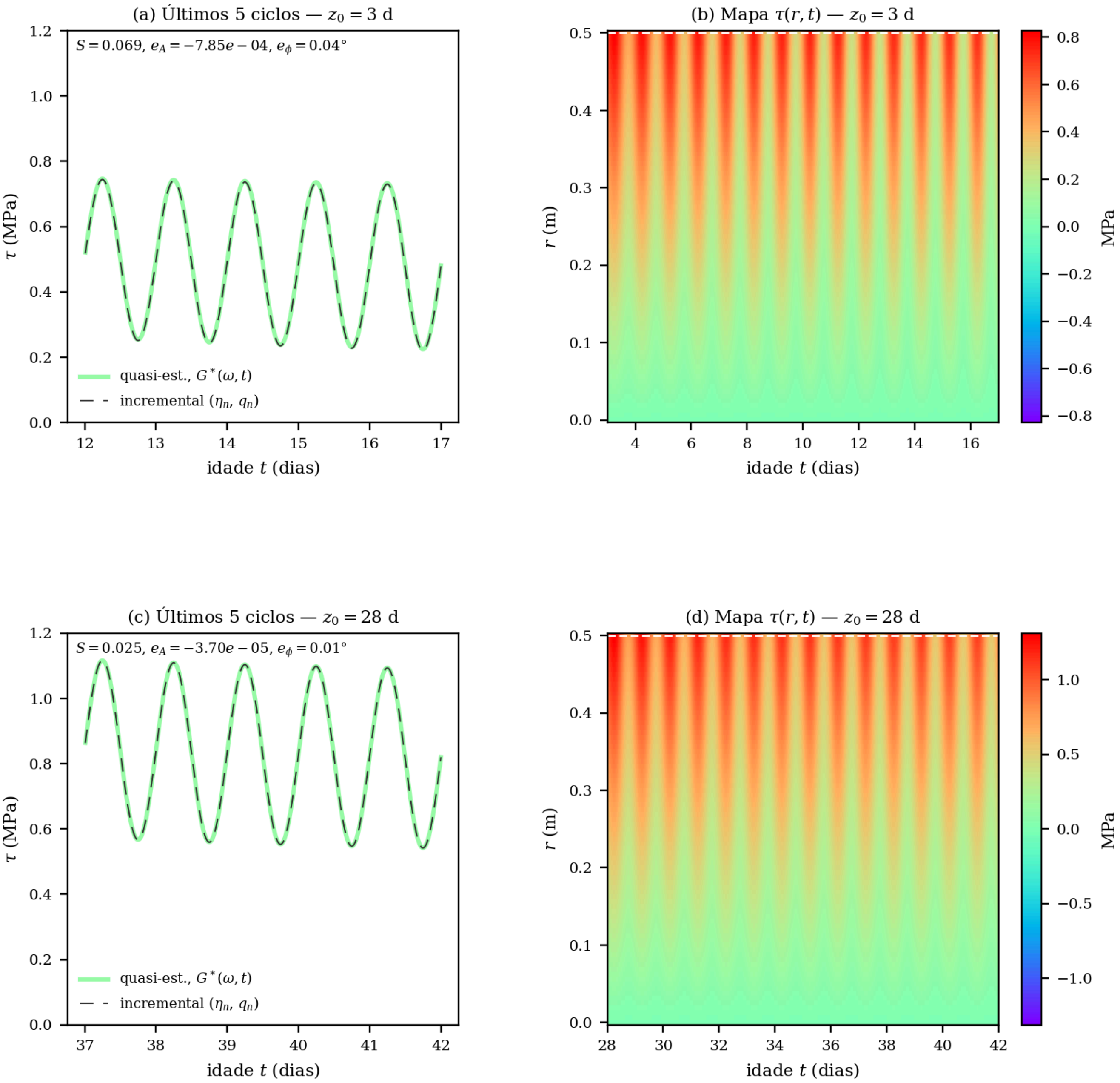

Figure 10 — Cylinder torsion, Case 2 ($R = 0.5$ m, $\kappa = 0.25$, $T = 1$ d): (a,b) $z_0 = 3$ d; (c,d) $z_0 = 28$ d — cuts at $r = R$ and maps $\tau(r,t)$.

8.3.4 Free slab under hydration — non-separable field

The second complementary test is purely thermal and opposite in structure to the previous one. The loading is $T(y,t)$ computed by finite differences (thickness $L = 1.5$ m, decreasing adiabatic generation, convection on the faces). Because the profile $T(y,\cdot)$ changes sign between heating and cooling, there is no separability $T = \theta(t)h(y)$; the response is obtained only by integrating step by step, with plane sections and null force and moment resultants at each instant — a *free* slab, distinct from the *restrained* slab of Section 9.2, which uses another thermal model ($L = 3$ m, Hill function) and restraint $\varepsilon_x = \varepsilon_y = 0$. Figure 11 brings the maps of $T(y,t)$ and $\sigma_1(y,t)$ and, below each, the cut at $y = 0$. In the stress panel, the hereditary reference by superposition with $R(t, t_k)$ and the incremental response appear superimposed (difference of 3.4×10^{-3} at the peak). There is tension at the surface and compression in the core after the thermal peak (maximum of 1.0 MPa on the face). The solver was verified separately with $T(y,t) = \theta(t)\cos(\pi y/L)$, a separable case with analytical reference (difference of 1.5×10^{-3} at the peak).

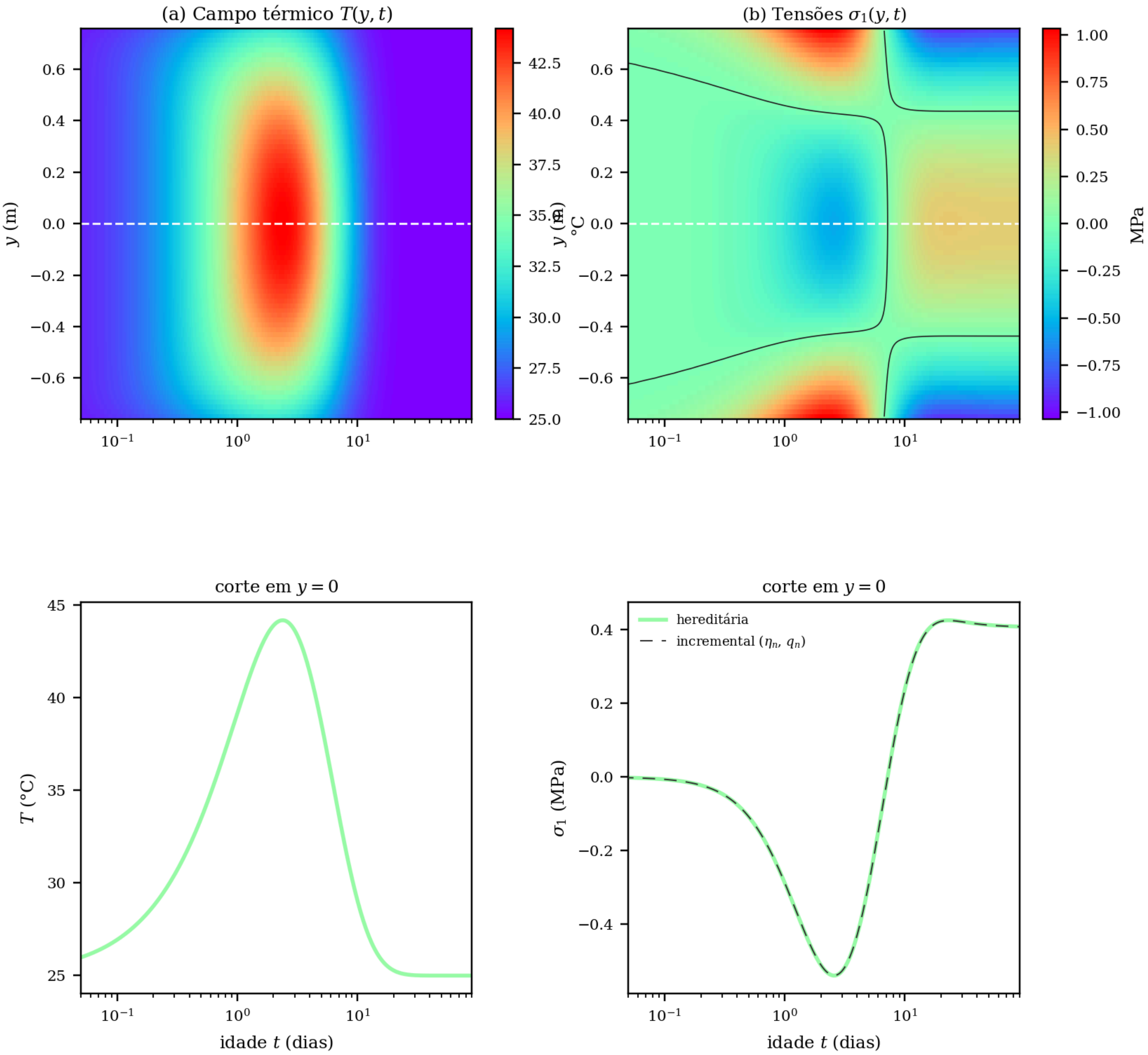

Figure 11 — Free slab under hydration ($L = 1.5\,\mathrm{m}$): (a) $T(y,t)$ and (b) $\sigma_1(y,t)$; below, cuts at $y = 0$ (hereditary via R × incremental in the stress panel).

Refining the time mesh uniformly in both cases, the algorithm error falls with order close to two when loading starts at an advanced age — 1.8 for $z_0 = 7$ days and 2.1 for $z_0 = 28$ days —, but falls only with order 1.1 when it starts at $z_0 = 1$ day. The maximum error is always located in the first step after loading. It is the numerical confirmation of what was recorded in Section 7.2: at early ages, $D_i(z)$ and $E(z)$ vary on the scale of the step itself, and the midpoint rule loses order.

8.4 Cylindrical hole under remote stresses

The previous cases are all thermal and therefore check the formulation from one side only. It is useful to close the validation with a case in which $\Delta T = 0$ and the loading is mechanical and held, because then Zhu's Theorem I (2014, §6.4) holds: the stresses are *not* affected by creep, and it is the strain that grows, at any point, by the factor $1 + E(\tau_0)C(t,\tau_0)$. It is the other side of the coin relative to Section 8.2, and ties directly to the instrumentation of Part II.

The problem is that of a cylindrical hole of radius a opened in an infinite medium subjected to a remote stress tensor, solved by Hiramatsu and Oka (1962) for the triaxial state. It is the generalized Kirsch for a three-dimensional body, in plane strain along the hole, with those authors' own contribution in the axial coupling: the component σ_ζ on the wall depends on ν and on the remote transverse stresses. Ruggeri and Gomes (2013) rewrote the solution in matrix form, in the notation adopted here. With $\eta = a/r$ and θ measured in the cross-section plane,

$$\left\{ \sigma_\theta,\, \sigma_\zeta,\, \tau_{\theta\zeta},\, \tau_{\zeta r},\, \tau_{r\theta},\, \sigma_r \right\}^T = \left[M(\nu, \theta, \eta) \right] \left\{ \sigma_x^\infty,\, \sigma_y^\infty,\, \sigma_z^\infty,\, \tau_{yz}^\infty,\, \tau_{zx}^\infty,\, \tau_{xy}^\infty \right\}^T,$$

with the coefficients m_{ij} given in that report. On the wall, $\eta = 1$ and $\sigma_r = \tau_{r\theta} = \tau_{\zeta r} = 0$ result, leaving the three components that the instrumentation reaches. The implementation was checked by three paths: the two equilibrium equations in polar coordinates, satisfied with residual of order 10^{-9}; the boundary conditions on the wall, exact; and the remote field, which for $r \gg a$ reproduces the rotation of the imposed tensor.

The layout of the problem is in Figure 12; Figure 13 gathers the results. One adopts $a = 1.5\,\mathrm{m}$, $\nu = 0.20$ and a remote tensor of -2.0, -1.2 and $-3.0\,\mathrm{MPa}$ in the normal directions, with shears of 0.4, -0.5 and $0.8\,\mathrm{MPa}$. The concentration takes σ_θ from $-1.9\,\mathrm{MPa}$ in the remote field to $-6.8\,\mathrm{MPa}$ on the wall, and there is a tensile zone of up to $0.4\,\mathrm{MPa}$ in the orthogonal direction. With the hole opened at age $z_0 = 28$ days and the loading held, the algorithm returns constant stress and strain equal to $\sigma_\theta J(t, z_0)$ with a difference of 4×10^{-16} — exact, not approximate, because the step is accounted for only by $\Delta D_{n,0}$, as shown in Section 6.3. On the wall, with $\sigma_r = 0$, the component $\varepsilon_r(t)$ follows $-\nu(\sigma_\theta + \sigma_\zeta)\, J(t, z_0)$ and confirms the same behaviour.

Furo cilíndrico em meio infinito sob tensor remoto triaxial

Hiramatsu e Oka (1962) — carregamento mecânico mantido, ΔT = 0 (Seção 8.4)

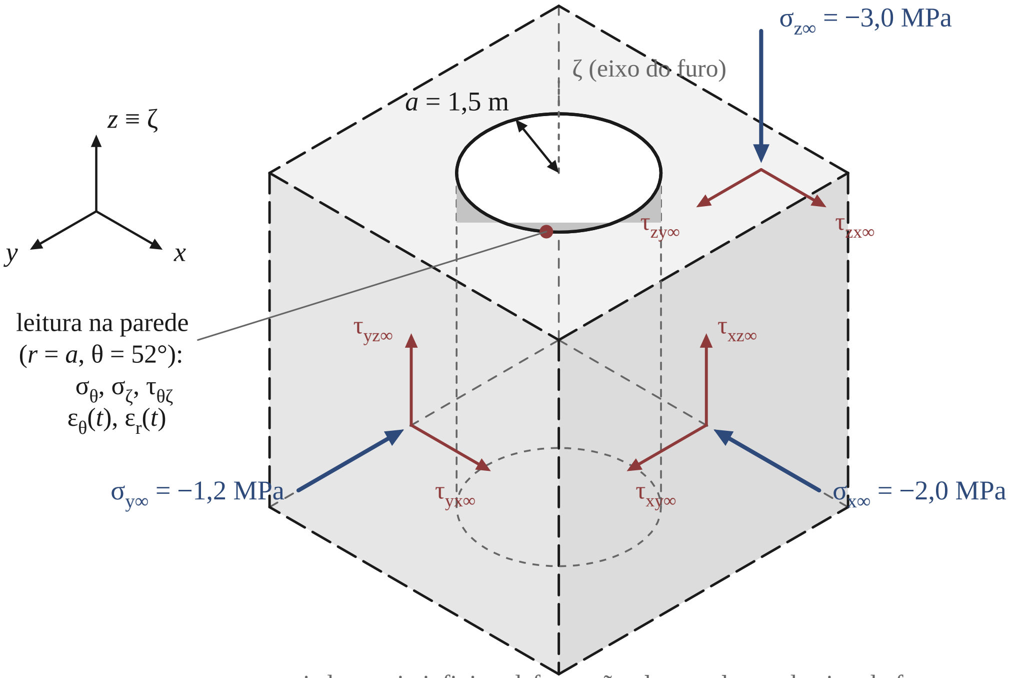

arestas tracejadas: meio infinito; deformação plana ao longo do eixo do furo
cisalhantes desenhadas no sentido positivo; valores no quadro abaixo

---

Geometria: furo cilíndrico de raio $a = 1{,}5$ m, eixo $\zeta \equiv z$, em meio infinito; $\eta = a/r$, θ no plano da seção.
Tensor remoto: $\sigma_{x\infty} = -2{,}0$; $\sigma_{y\infty} = -1{,}2$; $\sigma_{z\infty} = -3{,}0$ MPa; $\tau_{yz\infty} = 0{,}4$; $\tau_{zx\infty} = -0{,}5$; $\tau_{xy\infty} = 0{,}8$ MPa.
Contorno: parede livre: $\sigma_r = \tau_{r\theta} = \tau_{\zeta r} = 0$ em $r = a$; tensor remoto recuperado para $r \to \infty$.
Carregamento: furo aberto em $z_0 = 28$ dias, solicitação mantida; $\Delta T = 0$ (Teorema I de Zhu).
Material: $\nu = 0{,}20$; $E(z)$ e $D(t,z)$ da cadeia de Kelvin com envelhecimento (UHE Itumbiara).
Resposta: σ constante; $\varepsilon_\theta(t) = \sigma_\theta J(t,z_0)$ e $\varepsilon_r(t) = -\nu(\sigma_\theta+\sigma_\zeta)J(t,z_0)$ na parede, $\theta = 52°$.

Figure 12 — Layout of the cylindrical hole under remote stresses (Hiramatsu and Oka, 1962).

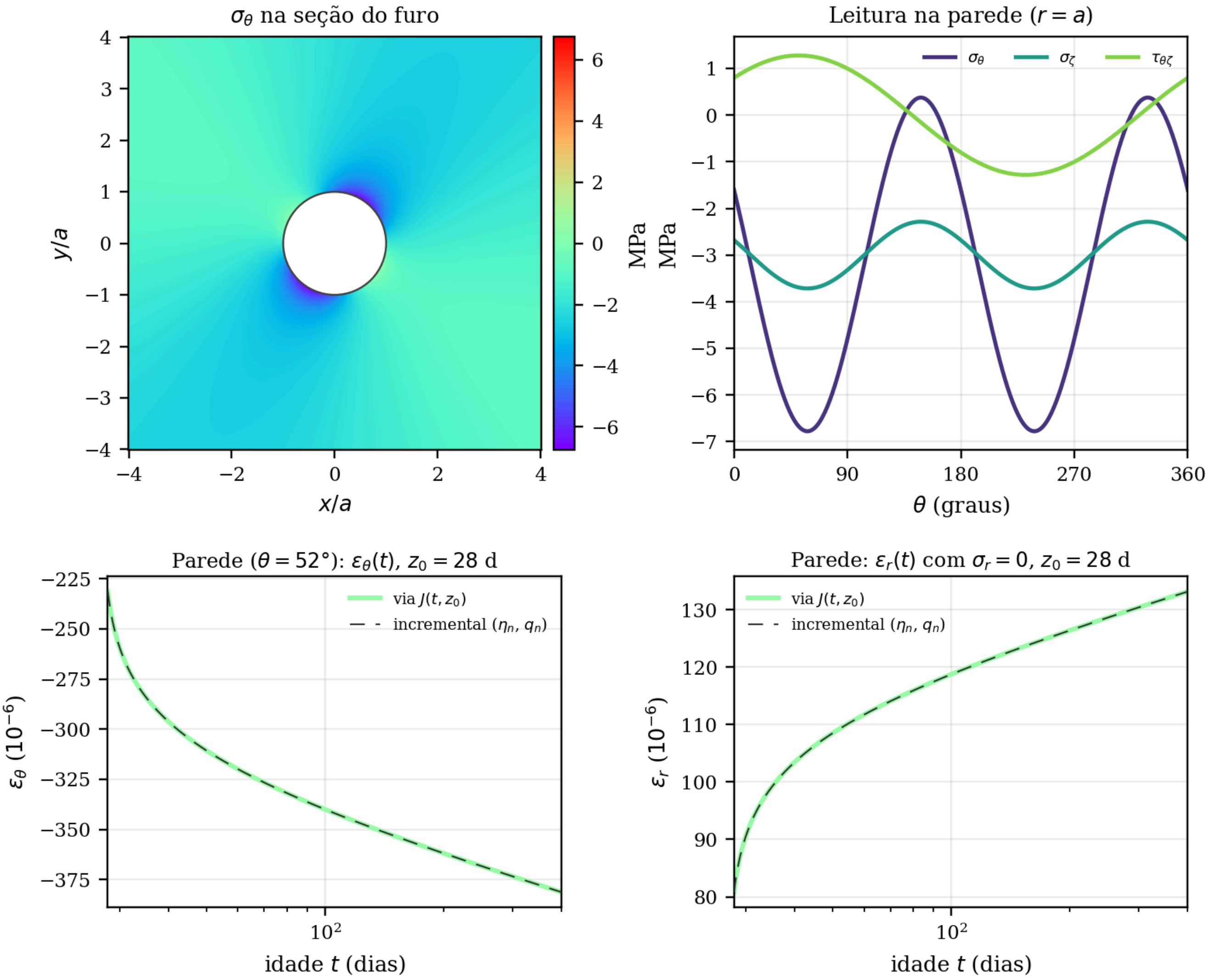

Figure 13 — Cylindrical hole under a triaxial remote tensor. Above: σ_θ on the cross-section (left) and the three components read on the wall (right). Below: $\varepsilon_\theta(t)$ and $\varepsilon_r(t)$ on the wall under held load from $z_0 = 28$ days (σ constant, strain by J).

There is a second reason to include this case. The experimental determination of the tensor from strains measured in chosen directions on the wall — the STT method, or the slots of the flat-jack method — is the same operation as the mass-concrete rosette: one assembles $\varepsilon_n = \widehat{n} \cdot \boldsymbol{\varepsilon} \cdot \widehat{n}$ for each direction and inverts the system. It is exactly where the distinction between γ_{ij} and ε_{ij} recorded in Section 2 corrupts the result if ignored. Going forth and back with four directions on the wall, the recovered tensor coincides with the imposed one to 6×10^{-14} in 10^{-6}. The check is trivial from the numerical standpoint and non-trivial from the assembly standpoint: it is the same routine that Part II applies to field readings.

9. Considerations on strain capacity

The literature treats under the same name two distinct things. The first is the strain-capacity test, in which a beam is taken to failure and the extreme-fibre strain at the instant of fracture is recorded. The second is the strain-capacity criterion, a verification rule used in thermal studies when that test is not available, and in which capacity is estimated from the modulus of rupture f_r and the elastic modulus E.

9.1 Classical criterion and stress equivalence

Houghton (1976) proposed estimating tensile strain capacity from routine tests. For rapid loading,

$$\varepsilon_{cap}^{r}(z) = \frac{f_r(z)}{E(z)}.$$

For slow loading, the increase due to creep leads to

$$\varepsilon_{cap}^{\ell}(t,z) = f_r(z)\, J(t,z),$$

or, with the creep coefficient $\varphi(t,z) = E(z)D(t,z)$,

$$\varepsilon_{cap}^{\ell}(t,z) = \varepsilon_{cap}^{r}(z)\left[1 + \varphi(t,z)\right].$$

On the demand side, a uniaxial state, a scalar restraint coefficient K_R and a temperature drop ΔT counted from the maximum temperature of the member are assumed:

$$\varepsilon_{dem}(t) = K_R\, \alpha_T\, \Delta T(t) \qquad \left[\, + \ \varepsilon^{shr} \text{ when present} \,\right].$$

The reference at $T_{\max}$ has documented origin. Carlson, Houghton and Polivka (1979) record that, at the instant of maximum internal temperature, "the stress is close enough to zero that it may be assumed to be zero". The physical reason is in the same text: during the temperature rise the concrete is "more or less plastic", and only after the peak does it become "stronger and approximately more elastic". It is a field observation, gathered from instrumented dams, and not a calculation result. The embedded instrument supplied strain and temperature; converting one into the other required precisely what was uncertain, the modulus at the loading age and the relaxation. The hypothesis therefore precedes the possibility of computing the stress history, and is not to be confused with the instant at which the computed stress is null — an instant that comes later, generally in cooling, when the compression accumulated in heating dissipates.

The classical verification is written

$$K_R\, \alpha_T\, \Delta T(t) \ \le\ \frac{\varepsilon_{cap}^{\ell}(t,z)}{\gamma},$$

in which γ is a safety factor. The most used design form is the allowable temperature drop, which Brazilian practice in thermal studies, especially in the Carlson/Houghton line, calls Equivalent Temperature Variation (EVT):

$$\Delta T_{adm}(t,z) = \frac{\varepsilon_{cap}^{\ell}(t,z)}{K_R\, \alpha_T} = \frac{f_r(z)\, J(t,z)}{K_R\, \alpha_T}.$$

It amounts to expressing strain capacity in temperature units: the allowable strain divided by $K_R \alpha_T$. Substituting $\varepsilon_{cap}^{\ell} = f_r J$ and dividing both sides by $J(t,z)$,

$$\frac{K_R\, \alpha_T\, \Delta T(t)}{J(t,z)} \ \le\ f_r(z) \qquad \Leftrightarrow \qquad \sigma_{ef}(t) \ \le\ f_r(z),$$

in which $\sigma_{ef} = K_R \alpha_T \Delta T\, E_{ef}$ and $E_{ef}(t,z) = 1/J(t,z)$ is the effective modulus. That is, the strain-capacity criterion is, term by term, a stress criterion with effective modulus. As a cracking index,

$$I(t) = \frac{f_r(z)}{\sigma_{ef}(t)} = \frac{\varepsilon^{\ell}_{cap}(t, z)}{\varepsilon_{dem}(t)}.$$

The slow-strain test route absorbs E, D and f_r into a single measurement. The stress-calculation routine requires the three pieces of information separately, but dispenses with the simplifying hypotheses of uniaxiality, of a scalar restraint coefficient (unless one wishes to simplify and approximate a 3D situation by a 1D one) and of a single loading age, which are built into the existence of a unique $J(t, z)$ in the denominator.

9.2 Restrained slab with aging and comparison of criteria

Zhu's *restrained slab* (2014, §7.1), with horizontal displacements prevented ($\varepsilon_x = \varepsilon_y = 0$), free face ($\sigma_z = 0$), is the same restraint state as the problem of Section 8.2, now with a continuous thermal history and elastic modulus varying with age. The situation falls within what is described by Zhu's Theorem II (null body force, non-null temperature variation, part of the boundary free and part with prescribed displacement), and therefore the displacements are those of the elastic structure. The relaxation-coefficient method (eq. (7.10) of Zhu) writes:

$$\sigma(t_n) = \sum_{i=1}^{n} \Delta\sigma^e_i\, K(t_n, \tau_i), \qquad \Delta\sigma^e_i = -\frac{E_i\, \alpha_T\, \Delta T_i}{1-\nu}, \qquad K(t,\tau) = \frac{R(t,\tau)}{E(\tau)},$$

with $E_i = \left[E(t_{i-1}) + E(t_i)\right]/2$ and $\tau_i = (t_{i-1} + t_i)/2$. $R(t, \tau)$ is obtained from J as in Section 8.2.1 (Zhu's empirical formula (7.13) is not used: the material is the same Kelvin chain with aging of Figures 4 and 5).

The temperature field adopted as an example is obtained from the temperature history at the centre point ($x = 1.5\,\mathrm{m}$) of a slab on ground (a typical foundation case). That history is obtained from a one-dimensional heat-conduction model of a slab of thickness $L = 3\,\mathrm{m}$, with internal generation (function called 'Hill') and convection on both faces. Adopted parameters: $T_0 = T_{\mathrm{amb}} = 20^{\circ}\mathrm{C}$; $k = 7.5\,\mathrm{kJ/(m \cdot h \cdot {}^{\circ}C)}$, $\rho = 2400\,\mathrm{kg/m^3}$ and $c = 0.75\,\mathrm{kJ/(kg \cdot {}^{\circ}C)}$, whence $h^2 = k/(\rho c) = 0.10\,\mathrm{m^2/d}$; $h_c = 43.2\,\mathrm{kJ/(m^2 \cdot h \cdot {}^{\circ}C)}$; adiabatic rise $\Delta T_{\mathrm{adi}} = 50^{\circ}\mathrm{C}$ with $\tau = 36\,\mathrm{h}$ and $\beta = 2$ (τ and β are kinetic parameters of the degree of hydration α); Arrhenius maturity with $E_a/R = 4000\,\mathrm{K}$ and $T_{\mathrm{ref}} = 20^{\circ}\mathrm{C}$. The peak at the centre results in $68^{\circ}\mathrm{C}$ at 2.5 days. In the restrained slab, $\sigma_x = \sigma_y$ at the point depends only on the *local* temperature; eq. (7.10) with $K = R/E$ is compared with the $\{\eta_n\}$, q_n algorithm, whose maximum difference on the mesh used is $0.034\,\mathrm{MPa}$ — about 1% of the peak value.

With the same temperature history, Figure 14 compares the stress and strain-capacity criteria of Section 9.1. Because the restraint is total ($\varepsilon_x = \varepsilon_y = 0$), $K_R = 1$ is adopted; the factor $(1-\nu)$ corresponds to the biaxial state of the slab, equivalent to the uniaxial state in which the classical criterion is written. Tensile strength evolves with maturity, $f_t = f_{t,\infty}\, t^n_{eq}/(a^n + t^n_{eq})$, with $f_{t,\infty} = 4.5\,\mathrm{MPa}$, $a = 2\,\mathrm{d}$ and $n = 1.2$.

In the upper-right plot (Figure 14) is the classical criterion: the demand is the drop $T_{\max} - T$ counted from the peak and the capacity is

$$\mathrm{EVT}(t) = \frac{f_t(t)\, J(t, z)\, (1-\nu)}{K_R\, \alpha_T}, \qquad z = t_{\max}.$$

EVT includes the elastic part of J and therefore starts from the plateau $f_t/E(z)$ at $t_{\max}$, not from zero. In the lower-right plot (Figure 14) is the adapted criterion: the same check rewritten in stresses,

$$\sigma_{ef}(t) = \frac{K_R\, \alpha_T\, (T_{\max} - T)_+}{(1-\nu)\, J(t, z)},$$

plotted from $t = 0$, null during heating and growing in cooling, and compared with $f_t(t)$. The two formulations are the same inequality, and indeed $T_{\max} - T \le \mathrm{EVT}$ and $\sigma_{ef} \le f_t$ change sign at the same instant, at 20 days.

It is of interest to compare those two panels with the lower left (Figure 14). Both writings of the classical criterion announce cracking at 20 days: at the end, $\sigma_{ef} = 5.76\,\mathrm{MPa}$ against $f_t = 4.48\,\mathrm{MPa}$. Incremental integration of the full history yields 5.47 MPa and also exceeds the strength. The difference comes from the two hypotheses of the classical route, null stress at the thermal peak and a single loading age $z = t_{\max}$, which leave out the compression accumulated during heating and the relaxation of increments applied at early ages.

It is useful to examine how those two hypotheses combine. In the example, the stress at the thermal peak is not null: it is $-6.45\,\mathrm{MPa}$ of compression. From the peak to the end of the simulation the stress varies by 11.9 MPa, whereas the estimate of that same variation by the effective modulus with a single age yields 5.76 MPa. The two deviations have opposite signs and largely compensate: $0 + 5.76 = 5.76$ against $-6.45 + 11.9 = 5.45$. The apparent agreement between σ_{ef} and the incremental stress in works with a similar history is due to that compensation, and not to the isolated accuracy of each hypothesis.

If, on the other hand, one knew the instant t^* at which the stress returns to zero after the compressive period — in the example, $t^* = 12.5$ days and $T^* = 46^\circ\mathrm{C}$ — and adopted that instant as the origin of the check, the thermal strain accumulated from t^* is the same on both routes: $\varepsilon_{dem}(t) = K_R \alpha_T (T^* - T)/(1-\nu)$ for $t \ge t^*$. The deviation between the light-blue dashed curve and the incremental stress in the lower-right panel of Figure 14 does not come from the thermal demand, but from the creep adopted in the denominator.

The naïve form $\sigma^*_{ef} = [K_R \alpha_T (T^* - T)_+]/(1-\nu)/J(t, t^*)$ applies a single $J(t, t^*)$ to the total temperature drop, as if the entire cooling had been imposed at once at t^*. That overestimates the creep time of each strain increment and therefore underestimates the stress — the curve exhibits more creep than the incremental one, although ε_{dem} is identical. The multi-age extension,

$$\sigma^*_{ef}(t) = \sum_{k:\ \tau_k \ge t^*} \frac{K_R\, \alpha_T\, \Delta T_k/(1-\nu)}{J(t, \tau_k)}, \qquad t \ge t^*,$$

assigns to each increment ΔT_k the J of its own age τ_k and tracks the incremental result closely in the first weeks (root-mean-square deviation of 0.22 MPa after t^*, against 0.54 MPa with a single J and 1.77 MPa with $z = t_{\max}$). The long-term residual (5.01 against 5.47 MPa at the end) reflects the memory state of the Kelvin chain at instant t^*: $\sigma(t^*) = 0$ does not imply a null viscoelastic history, and the previous compression continues to influence the subsequent tension.

Hence a recommendation of practical order: the two classical hypotheses ($\sigma = 0$ at $t_{\max}$ and single age $z = t_{\max}$) cannot be corrected separately. Keeping the computed peak compression and retaining the effective modulus with $z = t_{\max}$ yields $-0.69\,\mathrm{MPa}$, that is, the conclusion that there would be no tension. With $z = t^*$ and multi-age creep, the same criterion structure approximates the incremental stress, but t^* and the memory state at t^* are not design data: they emerge only from the full calculation or from instrumentation.

In histories of mild cooling and uniform restraint, σ_{ef} and the incremental stress track each other; the divergence in multi-age histories is the subject of Section 9.3.

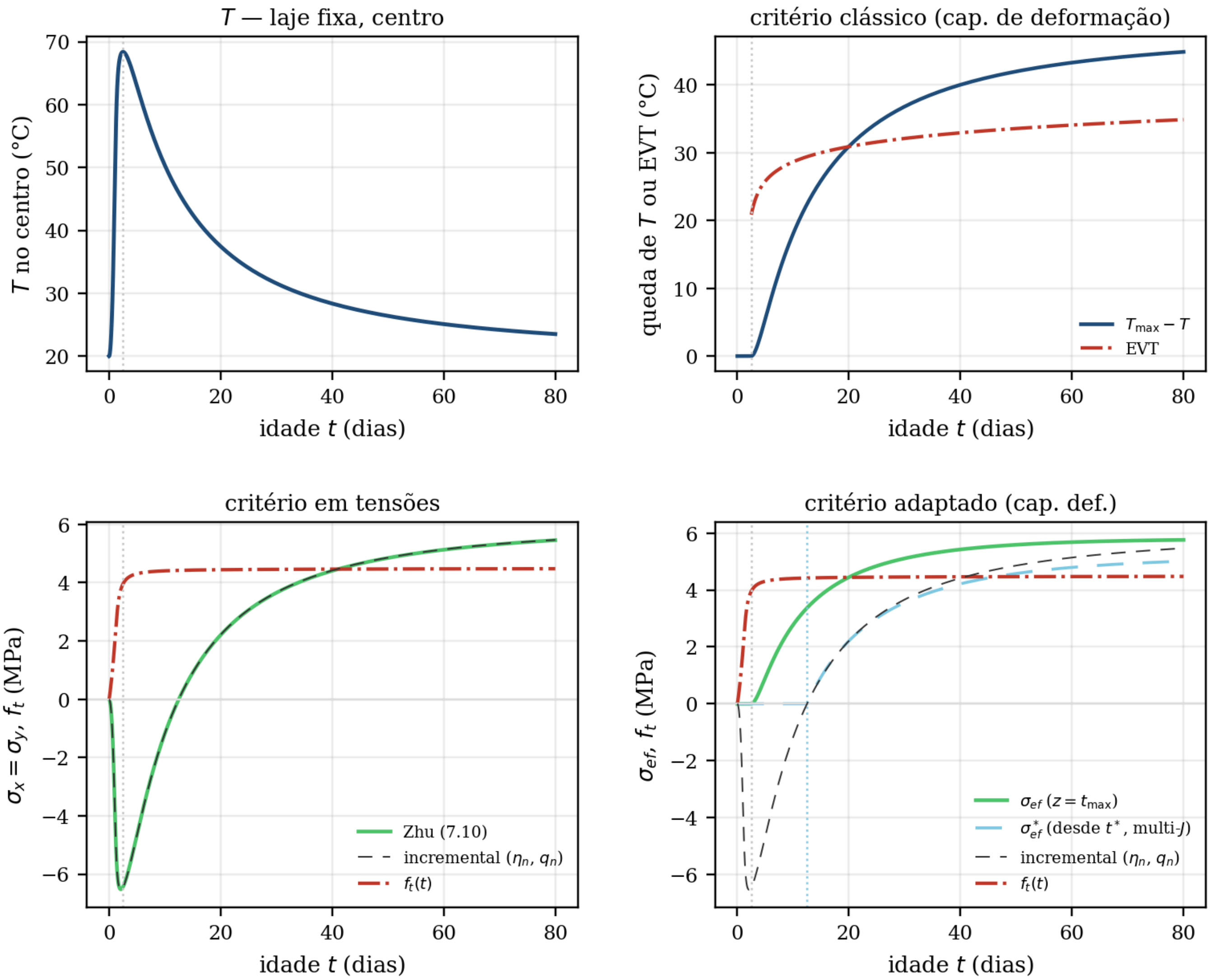

Figure 14 — Restrained slab with aging: top — T at the centre and classical criterion ($T_{\max} - T$ and EVT); bottom — stress criterion ($\sigma_x = \sigma_y$ via Zhu and via incremental, with f_t) and adapted criterion (σ_{ef} with $z = t_{\max}$; multi-J σ^*_{ef} from t^*, light-blue dashed).

9.3 Limit of validity and check with the incremental formulation

In a real thermal history there is no single loading age z: the stress is built by increments applied at all ages. There is therefore no unique $J(t, z)$, nor a unique effective modulus, and the identity above dissolves. The classical criterion remains exact only in the particular case of loading at a single age — which is precisely the situation of a test.

At this point, the incremental formulation of this paper comes into its own again. Taking as input the same $D_i(z)$, τ_i and $E(z)$, it returns the field $\{\sigma(t)\}$ throughout the structure, and the check becomes:

$$I(t) = \frac{f_t(t)}{\sigma_1(t)} \ \geq \ I_{adm},$$

with σ_1 the major principal stress. In that form, the elements of empirical nature are restricted to $f_t(t)$ and the threshold I_{adm}, each with its own meaning and with uncertainties that can be assessed separately.

Zhu (2014, §6.4 and §6.5) delimits that scope by another path. Alfrey had already treated the homogeneous structure under simple boundary conditions, with the boundary entirely under forces or entirely under prescribed displacements. Zhu extended the result to the *non-homogeneous* structure under mixed boundary, under the condition that the material constants be proportional,

$$E_1(\tau)\, C_1(t,\tau) = E_2(\tau)\, C_2(t,\tau), \qquad \mu_1 = \mu_2 = \mu,$$

and stated two theorems: Theorem II, used in Section 9.2, and Theorem I, taken up in Section 9.4. Both hold with aging, since E and C depend on age. They therefore go beyond the correspondence principle. Structures that satisfy that condition the author calls *proportional-deformation structures*: homogeneous member on a rigid foundation; non-homogeneous member on a rigid foundation with proportional constants; member and viscoelastic foundation with all constants proportional. In those cases the viscoelastic response comes from the elastic response by Theorem I or by the relaxation coefficient of Theorem II, without incremental integration, as was done in Section 9.2.

Outside that class the author himself then refers to the finite-element method (FEM). It is the case of concretes of non-proportional creeps due to contact, for example, of a concrete with the foundation rock, of lifts cast at different ages, and of boundaries that vary with the evolution of the work. For that other, more general domain, what was presented in the formulation of Sections 4 to 7 is valid. There too there are premises of validity, but it serves the general case in which the proportionality hypothesis does not hold.

9.4 Flexural creep test under held load

As an alternative to the destructive rapid-loading strain-capacity test, a flexural creep test is proposed in which the load is applied and held constant, without taking the specimen to failure. In a simply supported beam with third-point loading, the moment field is fixed by equilibrium; if the material is homogeneous and ages uniformly, the elastic stress distribution satisfies the equilibrium and compatibility conditions at any instant. It is not necessary to invoke the correspondence principle of Alfrey and Read, which requires a convolution kernel and does not hold with aging.

This is supported by Zhu's Theorem I (2014, §6.4), stated for aging material. For the homogeneous structure, or non-homogeneous with proportional material constants, with null temperature variation, part of the boundary under external force and part with prevented displacement, the stresses due to body forces and external forces *are not affected by creep*, and the strain at any point and instant is obtained from the elastic strain at the loading age τ_0 by

$$\varepsilon(x,y,z,t) = \varepsilon^{e}(x,y,z,\tau_0)\left[1 + E(\tau_0)\, C(t,\tau_0)\right].$$

The beam under held load is that case. The stress distribution remains the elastic one and the extreme-fibre strain grows by the factor $1+\varphi(t,\tau_0)$, that is, $\varepsilon(t)/\sigma_0 = J(t,\tau_0)$, which is the reading of the test.

Recording the extreme-fibre strain $\varepsilon(t)$ under constant stress σ_0 applied at age z_0,

$$J(t,z_0) = \frac{\varepsilon(t) - \varepsilon^{shr}(t)}{\sigma_0},$$

in which ε^{shr} comes from an unloaded companion beam, sealed under the same conditions. It is recommended that $\sigma_0 \le 0.4\, f_r(z_0)$ to remain in the linear range and avoid microcracking that adds non-linearities. Replicating the test at staggered ages $z_0^{(1)}, \ldots, z_0^{(K)}$, one builds the surface $D(t,z)$ and obtains the Kelvin-chain parameters, which are the input data of the formulation in Section 3.

From the algorithm standpoint, this test is the step $\{\Delta\sigma_0\}$ at $t_0 = z_0$ with $\{\Delta\sigma_n\} = \mathbf{0}$ for $n \ge 1$. Under that condition, Section 6 showed that the successive terms of the sum cancel in pairs and the result reproduces $J(t,z_0)$ exactly — the test therefore serves at once as calibration of the chain and as validation of the code before applying it to the thermal history.

10. Conclusions

In this work the derivation of the aging creep strain increment in the form $\{\Delta\varepsilon_n^{cr}\} = \{\eta_n\} + q_n[\mathbb{V}]\{\Delta\sigma_n\}$ was presented in detail. From the creep function D as a series of exponentials with age-dependent coefficients $D_i(z)$ and retardation times τ_i, under the hypothesis of constant stress rate in each step, one obtains the scalar q_n, the auxiliary variables $\{\omega_{i,n}\}$ and the hereditary vector $\{\eta_n\}$, without reintegrating from the origin.

It was verified, analytically and numerically, that under a stress step $\Delta\sigma_0$ applied at age z_0 and held constant, the algorithm reproduces exactly $D(t, z_0)$ and, with the elastic part, the creep compliance $J(t, z_0)$ itself, whatever the time discretization. The formulation sits aligned with the algorithmic approach of Zocher et al. (1997), but now anchored in the creep function with aging.

The incrementalization was validated in the limit without aging (Zocher et al.) and in plane stress, as well as in a restrained slab with aging (Zhu). With that, Part I closes the link between the derivation and the finite-element implementation.

It remains to delimit the scope: by Zhu's theorems for proportional-deformation structures, the viscoelastic response with aging comes directly from the elastic response, without incremental integration. That is the case of the homogeneous member on a rigid foundation and of the member and foundation with proportional material constants. The formulation presented does not replace that result within that scope of validity. It is intended for the general case, in which concretes of distinct creeps coexist in the same structure, the foundation is real and the boundary changes along construction, with formwork removal, changes in curing and environmental conditions — situations for which the author himself refers to the finite-element method.

Part II, in preparation, will treat the numerical–experimental validation of a mass concrete termed 'class J' of the Log Spillway (VET) at Santo Antônio HPP: comparison of FEM strains with embedment strain gauges, of the stress tensor from the rosette+stress-free box with those from the finite-element software, and of the *concrete stress meter* as a supporting reference, in reduced time via *shift factor* a_T.

11. References

ANDRADE, W. P. et al. (Furnas team). *Concretos: massa, estrutural, projetado e compactado com rolo — ensaios e propriedades*. São Paulo: Pini/Furnas, 1997.

GAMBALE, E. A.; FONTOURA, J. T.; GUEDES, Q. M.; PACELLI, W. A. Resolução numérica do modelo viscoelástico linear com envelhecimento do concreto e sua aplicação no cálculo das tensões de origem térmica em barragens de C.C.R. In: SEMINÁRIO NACIONAL DE GRANDES BARRAGENS, 20.; REUNIÃO DO IBRACON, 34., 1992, Curitiba. *Anais*... Curitiba: [s.n.], 1992.

GUEDES, Q. M.; GAMBALE, E. A. Modelos viscoelásticos com envelhecimento para o betão em massa de barragens. *Informação Científica Barragens*, Lisboa: Laboratório Nacional de Engenharia Civil, p. 1–7, 1990.

BAŽANT, Z. P. *Mathematical modeling of creep and shrinkage of concrete*. Chichester: John Wiley & Sons, 1988.

JIRÁSEK, M.; BAŽANT, Z. P. *Inelastic Analysis of Structures*. Chichester: John Wiley & Sons, 2002.

GOMES, F. M. P. Estudo da fluência do concreto massa — hidrelétricas mais seguras e sustentáveis. In: CONGRESSO BRASILEIRO DO CONCRETO, 55., 2013, Gramado. *Anais*... São Paulo: IBRACON, 2013.

QUEBEC ENGENHARIA / GST. *Relatório GST.E.051.2015-R0* — UHE Salto do Apiacás: estudos térmicos e tensionais unidimensional e bidirecional do concreto de 2º estágio. 2015.

CARLSON, R. W.; HOUGHTON, D. L.; POLIVKA, M. Causes and control of cracking in unreinforced mass concrete. *ACI Journal*, Proceedings v. 76, n. 7, p. 821–837, July 1979.

CARLSON, R. W.; HOUGHTON, D. L.; POLIVKA, M. Causas e controle de fissuração em concreto massa sem armadura. Translated by W. P. de Andrade. *Revista do Instituto Roy Carlson*, v. 1, n. 2, p. 1–11, 2026. (Portuguese translation of Carlson, Houghton and Polivka, 1979.)

CARMO, J. B. M.; ALI, E. Análise Térmica do Concreto da Barragem Canoas. In: SEMINÁRIO NACIONAL DE CCR, 2., 1996, Curitiba. *Anais*... São Paulo: IBRACON, 1996. v. 1.

CARMO, J. B. M.; ALI, E. Uma Metodologia para Análise de Temperatura no CCR. In: SEMINÁRIO NACIONAL DE GRANDES BARRAGENS, 23., 1999, Belo Horizonte. *Anais*... Rio de Janeiro: CBGB, 1998. v. 1.

HOUGHTON, D. L. Determining tensile strain capacity of mass concrete. *ACI Journal*, v. 73, n. 12, p. 691–700, Dec. 1976.

HOUGHTON, D. L. Concrete strain capacity tests — their economic implications. In: ENGINEERING FOUNDATION RESEARCH CONFERENCE ON ECONOMIC CONSTRUCTION OF CONCRETE DAMS, 1972, Pacific Grove, California. *Proceedings*... p. 75–99.

BAŽANT, Z. P.; HUBLER, M. H.; WENDNER, R. RILEM draft recommendation: TC-242-MDC multi-decade creep and shrinkage of concrete — material model and structural analysis. *Materials and Structures*, v. 48, p. 753–770, 2015.

BAŽANT, Z. P.; PRASANNAN, S. Solidification theory for concrete creep. I: formulation; II: verification and application. *Journal of Engineering Mechanics*, v. 115, n. 8, p. 1691–1725, 1989.

BAŽANT, Z. P.; XI, Y. Continuous retardation spectrum for solidification theory of concrete creep. *Journal of Engineering Mechanics*, v. 121, n. 2, p. 281–288, 1995.

JIRÁSEK, M.; HAVLÁSEK, P. Accurate approximations of concrete creep compliance functions based on continuous retardation spectra. *Computers and Structures*, v. 135, p. 155–168, 2014.

ZOCHER, M. A.; GROVES, S. E.; ALLEN, D. H. A three-dimensional finite element formulation for thermoviscoelastic orthotropic media. *International Journal for Numerical Methods in Engineering*, v. 40, n. 12, p. 2267–2288, 1997.

SOUZA, F. V.; ALLEN, D. H. Multiscale modeling of impact on heterogeneous viscoelastic solids containing evolving microcracks. *International Journal for Numerical Methods in Engineering*, v. 82, n. 4, p. 464–504, 2010.

SOUZA, F. V.; ALLEN, D. H. Modeling the transition of microcracks into macrocracks in heterogeneous viscoelastic media using a two-way coupled multiscale model. *International Journal of Solids and Structures*, v. 48, n. 22–23, p. 3160–3175, 2011.

SOUZA, F. V. *Multiscale modeling of impact on heterogeneous viscoelastic solids with evolving microcracks*. 2009. PhD thesis (Engineering Mechanics) — University of Nebraska-Lincoln, Lincoln, 2009.

BAŽANT, Z. P. Numerical determination of long-range stress history from strain history in concrete. *Materials and Structures*, v. 5, p. 135–141, 1972.

ZHU, Bofang. *Thermal stresses and temperature control of mass concrete*. Oxford: Butterworth-Heinemann, 2014.

TIMOSHENKO, S. P.; GOODIER, J. N. *Theory of elasticity*. 3rd ed. New York: McGraw-Hill, 1970.

HIRAMATSU, Y.; OKA, Y. Stress around a shaft or level excavated in ground with a three-dimensional stress state. *Memoirs of the Faculty of Engineering, Kyoto University*, v. 24, Part 1, p. 56–76, 1962.

RUGGERI, E. R. F.; GOMES, F. M. P. *Tensões "in situ" em maciços rochosos*. Technical report. Goiânia: Eletrobrás Furnas, Feb. 2013.

GOMES, F. M. P. *Monitoramento do VET da UHE Santo Antônio — execução e resultados*. Technical report (experimental campaign, class J concrete). ANEEL/FURNAS Project, 2014. (unpublished)

SASSONE, M.; CHIORINO, M. A. Calculations of long-term structural behaviour of concrete structures. In: *Proceedings of the Workshop on Creep, Shrinkage and Durability of Concrete and Concrete Structures*, 2005.

GOMES, F. M. P.; SOUZA, F. V. Cálculo de tensões de origem térmica no concreto massa considerando fluência com envelhecimento — Parte II: validação numérico-experimental no VET da UHE Santo Antônio. *Revista do Instituto Roy Carlson*, v. 1, n. 2, 2026. (in preparation).

12. Annex A — List of symbols

Symbol	Meaning
$J(t, z)$	Total creep compliance: strain per unit stress at t for load applied at age z
$D(t, z)$	Creep part proper, $J(t, z) - 1/E(z)$; $D(z, z) = 0$
$D_i(z)$	Amplitude of the i-th Kelvin-chain element, dependent on loading age
$D^*_{i,n}$	Value of D_i at the midpoint of step n: $D_i(t_n - \Delta t_n/2)$
τ_i	Retardation time of the i-th chain element ($i = 1, \ldots, N$)
N	Number of Kelvin units in the chain
M_i	Number of aging exponentials of the i-th unit
a_i, $b_{i,j}$, $c_{i,j}$	Coefficients of the form $D_i(z) = a_i + \sum_{j=1}^{M_i} b_{i,j} e^{-z/c_{i,j}}$
$\Delta D_{n,z}$	$D(t_n, z) - D(t_{n-1}, z)$; with $z = t_0$, written $\Delta D_{n,0}$
$\mathbb{V}$, $[\mathbb{V}]$	Isotropic spatial operator with elastic Poisson ratio (4th-order tensor and Voigt matrix with $\gamma_{ij} = 2\varepsilon_{ij}$)
$E(z)$	Elastic modulus at age z
ξ, ξ'	Reduced times corresponding to t and z (the prime on ξ' denotes loading age)
a_T	*Shift factor* of the time–temperature superposition principle
h^2	Thermal diffusivity, $h^2 = k/(\rho c)$
α	Degree of hydration (reaction progress; Hill-type generation)
α_T	Coefficient of thermal expansion
$\{\Delta\sigma_0\}$	Stress step applied at t_0
$\{\Delta\sigma_n\}$	Stress increment in step n (continuous part of the history)
q_n	Scalar coefficient of the current step
$\{\omega_{i,n}\}$	Auxiliary memory variable of the i-th term of the series
$\{\eta_n\}$	Hereditary part known at the beginning of the step

13. Annex B — Obtaining the Kelvin chain

Section 3 takes the Kelvin chain with aging as given. This annex treats where it comes from: how to determine the retardation times τ_i and the amplitudes $D_i(z)$ from a predictor model or from test data, which constraints the creep surface must respect, and why, in the case of model B4, that work need not be done by regression.

13.1 The problem

The formulation of Sections 4 to 7 requires that $D(t, z)$ be a finite sum of exponentials in the load duration, with retardation times common to all stress increments. It is the fact that the τ_i are fixed that allows factoring the internal state into the variables $\{\omega_{i,n}\}$ and obtaining the recurrence of constant cost per step; and it is the dependence of D_i only on z that preserves the linearity of superposition.

Given a creep predictor, the problem is to determine $\{\tau_i, D_i(\cdot)\}$ that reproduces the family of curves with a residual small enough not to contaminate the stress calculation. The answer depends on a property of the predictor.

13.2 Separable models: exact fit in two stages

A predictor is separable when the specific creep is the product of a function of age by a kernel that depends only on duration,

$$D(t, z) = \varphi(z)\, K(t - z).$$

That is the case of ACI 209, whose kernel has the form $K(u) = u^{\psi}/(d + u^{\psi})$ and whose age dependence enters by a multiplicative factor.

Separability decomposes the fit into two independent problems, each of them one-dimensional and which can therefore be driven to arbitrary precision. In the first stage the kernel is fitted, $K(u) \approx \sum_i \phi_i \left(1 - e^{-u/\tau_i}\right)$; in the second, the aging law, $\varphi(z) \approx a + \sum_j b_j e^{-z/c_j}$. The result is the product, $D_i(z) = \phi_i\, \varphi(z)$, and the total error is the sum of two errors that are controlled separately. The key is that age enters only as a common vertical scale factor for all units: the shape of the curve in duration is the same for every loading age.

13.3 Admissibility of the creep surface

Two conditions matter. The first is monotonicity: creep grows with duration and decreases with loading age,

$$\frac{\partial J}{\partial t} \geq 0, \qquad \frac{\partial J}{\partial z} \leq 0.$$

The second is the non-divergence condition,

$$\frac{\partial^2 J(t, z)}{\partial t\, \partial z} \;\geq\; 0,$$

which requires that the creep curves of distinct loading ages, plotted against current time, not diverge from each other. It is not a strict thermodynamic requirement, but it is satisfied by experimental data and is a sufficient condition for the relaxation modulus obtained by superposition to be non-negative and monotonic — which matters directly here, since R is obtained from J by the recurrence of Section 8.2.1.

Applied to the form of Section 3, non-divergence supplies a criterion by part. From

$$\frac{\partial^2 D}{\partial t\, \partial z} = \sum_i e^{-(t-z)/\tau_i} \left[\frac{D_i'(z)}{\tau_i} + \frac{D_i(z)}{\tau_i^2} \right]$$

it follows that term-by-term positivity is equivalent to

$$\tau_i \;\leq\; \frac{D_i(z)}{-D_i'(z)}$$

for every age z of interest. For the usual form $D_i(z) = a_i + b_i e^{-z/c_i}$ with $a_i, b_i \geq 0$, the criterion reduces, in the case $a_i = 0$, to the condition $\tau_i \leq c_i$: the characteristic decay time of the amplitude cannot be smaller than the retardation time of the unit. The criterion is sufficient and not necessary — the sum may be admissible with isolated parts violating it —, but it serves as a precise diagnosis, applicable unit by unit on the assembled chain.

It is useful to record the result of that diagnosis on the usual predictors, evaluated before any fit, on a grid of eight ages by six durations: ACI 209 violates non-divergence at 24 of the 48 points, the US Bureau at 27, and B4 at none. That is not a reason to discard the first two, whose usefulness in a preliminary study remains, but it explains why the chain fitted to them so often produces a negative relaxation modulus at young ages: the inadmissibility is already in the target, and the fit merely transports it.

13.4 Model B4 and the exact spectral representation

The basic creep of B4 under sealed conditions keeps the form of B3,

$$J(t,z) = q_1 + q_2\,Q(t,z) + q_3 \ln\left[1 + (t-z)^n\right] + q_4 \ln\frac{t}{z}, \qquad n = 0.1.$$

The three time-dependent parts correspond to viscoelastic creep with aging, viscoelastic creep without aging and flow, deduced from solidification theory. They are not three empirical kernels chosen for convenience, and it is from that difference of nature that the failure of treating them as if they were of the same type follows.

B4 is not separable, and no amount of additional terms in the aging law corrects that. The q_4 part illustrates the reason. Writing $u = t - z$, one has $q_4 \ln(t/z) = q_4 \ln(1 + u/z)$, which is a horizontal translation on the logarithmic axis of duration, with a shift factor proportional to z. A logarithmic shift is additive, not multiplicative: the ratio between the curve of z and that of a reference age depends on u , and not weakly. With $z_{ref} = 7$ d and $z = 0.5$ d it equals 8.23 for $u = 1$ d, 3.44 for $u = 10$ d and 1.97 for $u = 91$ d. There is no $D(z)$ capable of absorbing a factor-of-four variation within an ordinary duration window.

The way out is to transfer the shift to the amplitudes, not as a common multiplicative factor, but as a spectral redistribution. In that form the result is exact.

13.4.1 Flow part

Frullani's identity supplies, for $z > 0$ and $u \geq 0$,

$$\int_0^\infty \left(1 - e^{-u/\tau}\right) e^{-z/\tau}\,\frac{\mathrm{d}\tau}{\tau} = \ln\left(1 + \frac{u}{z}\right).$$

Recognizing $\mathrm{d}\tau/\tau = \mathrm{d}\ln\tau$, this says that the flow part has an exact continuous retardation spectrum $\mathfrak{L}^{(4)}(\tau,z) = q_4\,e^{-z/\tau}$. Discretizing with constant geometric ratio X between neighbouring retardation times,

$$D_i^{(4)}(z) = q_4 \ln X\, e^{-z/\tau_i},$$

that is, the form $a_i + b_i e^{-z/c_i}$ adopted in Section 3 is exactly the correct form for this part, with $a_i = 0$, $b_i = q_4 \ln X$ equal for all units and $c_i = \tau_i$. There is no parameter to fit.

Two numerical consequences deserve recording, because they run counter to current practice. The spectrum tends to q_4 as $\tau \to \infty$: it does not decay — it tends to the constant q_4. Truncating the τ window at the maximum analysis duration costs about $q_4\,u/\tau_{\max}$, which for $u = 91$ d and $\tau_{\max} = 10^4$ d represents nearly 1% — an error that no least-squares algorithm eliminates and that it redistributes among the other parts, contaminating the entire fit. The window must extend to 10^6 or 10^7 days. And the usual half-decade spacing is coarse for this part: going to four units per decade, the error falls from 0.22% to about 10^{-2}%.

There is still a point that explains a known symptom. Because $\partial J^{(4)}/\partial t = q_4/t$ does not depend on z, one has $\partial^2 J^{(4)}/\partial t\,\partial z \equiv 0$: this part sits exactly on the non-divergence boundary, with no slack. Any fitting error that produces c_i slightly smaller than τ_i pushes the unit to the inadmissible side. Because, in addition, the age sensitivity $-\partial J^{(4)}/\partial z = q_4/z$ diverges as $z \to 0$, one understands why negative relaxation moduli appear preferentially at $z = 0.5$ and $z = 1$ day. Imposing the identity above, instead of regressing the aging law of this part, removes that source of inadmissibility by construction.

13.4.2 Viscoelastic part with aging

There remains the $q_2 Q$ part, defined by the solidification integral

$$q_2\, Q(t,z) = \int_z^t \psi(s)\, \Phi^{'}(s-z)\, \mathrm{d}s, \qquad \Phi(\xi) = \ln\left(1+\xi^n\right), \qquad \psi(s) = q_2 \left(\frac{\lambda_0}{s}\right)^m,$$

with $\lambda_0 = 1$ day and $m = 1/2$. It is the only genuinely non-separable one, and it too admits an exact representation.

Theorem. Let ψ and $\Phi^{'}$ be completely monotone, with Bernstein representations $\psi(s) = \int_0^\infty \rho(w) e^{-sw}\,\mathrm{d}w$ and $\Phi^{'}(\xi) = \int_0^\infty \ell(\sigma) e^{-\xi/\sigma}\,\mathrm{d}\sigma$, with $\rho, \ell \geq 0$. Then, with $u = t - z$,

$$C(t,z) = \int_{-\infty}^{+\infty} \mathfrak{L}(\tau, z)\left[1 - e^{-u/\tau}\right]\, \mathrm{d}\ln\tau,$$

with non-negative spectral density given in closed form by

$$\mathfrak{L}(\tau,z) = \int_\tau^\infty \ell(\sigma)\, \rho\left(\frac{1}{\tau} - \frac{1}{\sigma}\right) \exp\left[-z\left(\frac{1}{\tau} - \frac{1}{\sigma}\right)\right] \mathrm{d}\sigma.$$

The proof is short. Writing $s = z + \xi$ and substituting the two representations, the inner integral in ξ equals $\tau\left(1 - e^{-u/\tau}\right)$ with $1/\tau = w + 1/\sigma$. Changing, at fixed σ, the variable w to τ, one has $\mathrm{d}w = \mathrm{d}\ln\tau/\tau$, and the factor τ of the inner integral cancels the $1/\tau$ of the Jacobian. The domain $w > 0$ corresponds to $\tau < \sigma$, which fixes the lower limit.

Three consequences matter to this paper.

The first is that loading age appears exclusively through the factor e^{-zw}, with $w = 1/\tau - 1/\sigma > 0$. The amplitude of each unit is therefore a continuous superposition of decaying exponentials in z, with non-negative coefficients and no constant term. The family $D_i(z) = a_i + b_i e^{-z/c_i}$ adopted empirically in Section 3 is the exact family, and the practice of fixing $a_i = 0$ in the first part finds its justification here.

The second is that admissibility is automatic. The time constants are $c = 1/w$ and the retardation times are $\tau = 1/(w + 1/\sigma)$, whence $c > \tau$ for every finite σ: every component strictly satisfies the admissibility criterion above. Equality occurs only in the limit $\sigma \to \infty$, which corresponds to a pure dashpot — that is, to the flow part. The two parts of B4 are members of the same family, and the flow part is the extreme case, the only one that touches the boundary.

The third is a limitation of principle. The spectrum in c associated with each retardation time is a continuum that extends from τ to infinity. Representing it by a single pair (b_i, c_i) per unit is a severe reduction, and it is from that that the irreducible residual observed in direct regressions of the family of curves comes. It is not a lack of terms: it is the single-amplitude form that cannot carry the target.

For $\psi(s) = q_2 \lambda_0^m s^{-m}$ the Bernstein representation is elementary, $\rho(w) = q_2 \lambda_0^m w^{m-1}/\Gamma(m)$, so that, having previously represented the non-aging kernel by $\Phi^{'}(\xi) = \sum_k (g_k/\sigma_k) e^{-\xi/\sigma_k}$, the density becomes an explicit finite sum,

$$\mathfrak{L}^{(2)}(\tau, z) = \frac{q_2 \lambda_0^m}{\Gamma(m)} \sum_{k:\, \sigma_k > \tau} \frac{g_k}{\sigma_k} w_k^{m-1} e^{-z w_k}, \qquad w_k = \frac{1}{\tau} - \frac{1}{\sigma_k},$$

with $m = 1/2$ and $\Gamma(1/2) = \sqrt{\pi}$. The structure is two-level: the chain $\{g_k, \sigma_k\}$ fits the non-aging kernel $\ln(1 + \xi^{0.1})$, which is a one-dimensional problem solvable to arbitrary precision, and the formula above does the rest with no additional fitting. Aging is not fitted; it is computed.

A numerical care is decisive. The exponent $m - 1 = -1/2$ produces an integrable singularity as $\tau \to \sigma_k^-$, and at elevated ages the factor e^{-zw} concentrates the spectral mass in a narrow neighbourhood immediately below each σ_k. Integrating directly in the variable τ, over cells of fixed logarithmic width, loses that mass: in a trial with four units per decade and $z = 91$ d the error thus committed reached -74%, which one might confuse with a failure of the representation. The quadrature must be done in the variable w, where the mass and the singularity are explicit, and the substitution $w = v^2$ eliminates the singularity exactly for $m = 1/2$.

13.4.3 Complete procedure

Gathering the four terms, regression of the family of curves is dispensable:

part	treatment
q_1	elastic, age-independent; $E = 1/q_1$ constant in the constitutive equation
q_3	non-aging kernel; amplitudes $q_3 g_i$, constant in z
q_4	exact spectrum $q_4 e^{-z/\tau}$; closed amplitudes $q_4 \ln X\, e^{-z/\tau_i}$
q_2	exact spectrum of the formula above; amplitudes by quadrature in w

The three chains are gathered by concatenation, since the sum of Kelvin chains is a Kelvin chain and the formulation of Sections 4 to 7 does not distinguish the origin of each unit — only the number of internal variables increases. Note the consequence of the first item: in B4 the elastic modulus does not age, and the apparent aging of the static modulus is an output of the model, recovered as $E(z) \approx 1/J(z + \Delta, z)$. Maintaining simultaneously an independent $E(z)$ law, imported from the thermal characterization, double-counts the same aging.

The implementation used in this work builds the chain with four units per decade from 10^{-4} to 10^{7} days, which results in $N = 45$ units after spectrum compression. The relative error against the predictor remains at 0.19% maximum and 0.03% on average, and falls under refinement of the spacing — behaviour characteristic of quadrature error, not of representation error.

13.5 The regression route and its scope

When the predictor does not admit a closed representation, or when the input is test data, regression remains. It is legitimate, but its scope needs to be stated, and it is smaller than is often supposed.

The table below compares, for the same B4 material, the maximum relative error of the chain against the predictor, as a function of loading age, by the two routes. The regression was conducted on an age mesh from 0.5 to 91 days.

z (d)	regression	exact spectrum
0.25	38 %	0.3 %
0.5	7 %	0.2 %
1	6 %	0.2 %
7	3 %	0.2 %
28	4 %	0.2 %
91	6 %	0.2 %
180	35 %	0.7 %

Within the fitted mesh the regression stays in the 3 to 7 % range; outside it the error rises by an order of magnitude. The behaviour is that expected of an extrapolation, and is not correctable by increasing the number of units, for the reason given above in the viscoelastic part. Two recommendations follow. The age mesh of the fit must cover all loading ages that the thermal history will actually solicit, which in mass concrete means starting at a fraction of a day. And the result must be submitted to the admissibility diagnosis above, unit by unit, before feeding the stress calculation.

The regression fit of the family of curves with aging remains, in the present state of this work, the least satisfactory part of the procedure, and is under review. The exact route, when applicable, should be preferred.

---

1. One adopts $[\mathbb{V}]$ whenever working in matrix form (Voigt column vectors) and $\mathbb{V}$ when emphasizing the tensor form. The physical operator is the same, yet **the Voigt matrix representation and the second-order tensor are not the same object** in the shear components — a distinction often omitted and which, if ignored, corrupts directional strains and the assembly of the rosette (Jirásek and Bažant, 2002).

   In the *engineering* Voigt convention adopted in this article, the column vectors read

   $$\{\varepsilon\} = \left\{\, \varepsilon_x,\, \varepsilon_y,\, \varepsilon_z,\, \gamma_{xy},\, \gamma_{yz},\, \gamma_{zx} \,\right\}^T, \qquad \{\sigma\} = \left\{\, \sigma_x,\, \sigma_y,\, \sigma_z,\, \tau_{xy},\, \tau_{yz},\, \tau_{zx} \,\right\}^T,$$

   with the engineering shear strain $\gamma_{ij} = 2\varepsilon_{ij}$ $(i \neq j)$, whereas the symmetric tensor $\boldsymbol{\varepsilon}$ holds the tensorial components ε_{ij}. Hence the factor $2(1+\nu)$ on the shear diagonal of $[\mathbb{V}]$: it is consistent with $\{\varepsilon\} = D\,[\mathbb{V}]\{\sigma\}$ in Voigt, and does *not* authorize treating the last three entries of $\{\varepsilon\}$ as if they were ε_{xy}, ε_{yz}, ε_{zx} in a tensorial operation.

   In particular, the strain in the unit direction $\widehat{n}$ is always the *tensorial* quadratic form

   $$\varepsilon_n = \widehat{n} \cdot \boldsymbol{\varepsilon} \cdot \widehat{n} = n_i\, \varepsilon_{ij}\, n_j,$$

   or, expanded,

   $$\varepsilon_n = \varepsilon_x n_x^2 + \varepsilon_y n_y^2 + \varepsilon_z n_z^2 + \gamma_{xy}\, n_x n_y + \gamma_{yz}\, n_y n_z + \gamma_{zx}\, n_z n_x$$

   (with $\gamma_{ij} = 2\varepsilon_{ij}$). If one assembles a "tensor" by placing γ_{xy} in the place of ε_{xy} and still applies $\widehat{n} \cdot \boldsymbol{\varepsilon} \cdot \widehat{n}$ as if the entries were tensorial, shear enters twice and the directional strain — and, consequently, the tensor recovered from the rosette — come out wrong. The practical rule is therefore: (i) incremental constitutive algorithm in Voigt, with $[\mathbb{V}]$ above; (ii) directional projections, eigenvalues and assembly/inversion of the rosette on the tensor ε_{ij}, converting $\varepsilon_{ij} = \gamma_{ij}/2$ on the way in and $\gamma_{ij} = 2\varepsilon_{ij}$ on the way out. ↩